Diploma Thesis

Molecular analysis of the tumor suppressor gene A20/TNFAIP3 in lymphoid malignancies

Markus Lassnig

CENTER FOR CLINICAL RESEARCH

Molecular analysis of the tumor suppressor gene A20/TNFAIP3 in lymphoid malignancies

Diploma Thesis

at

Graz University of Technology

submitted by

Markus Lassnig

Institute for Genomics and Bioinformatics
Graz University of Technology
A 8010 Graz, Austria

Assessor: Scheideler, Marcel, Dipl.-Chem. Dr.rer.nat.

Advisor: Neumeister, Peter, Ao.Univ.-Prof. Dr.med.univ.

October 12, 2011

Graz University of Technology

Danksagung

Diese Arbeit bietet mir nicht nur die Möglichkeit, meine interessante interdisziplinäre Arbeit des letzen Jahres zu dokumentieren, sondern eröffnet mir darüber hinaus die Gelegenheit, den Menschen zu danken, die zum Erfolg dieser Arbeit beigetragen haben. Mein besonderer Dank gilt meinem Erstbetreuer ao. Univ. -Prof. Dr. med. univ. Peter Neumeister sowie meinem Co-Betreuer Mag. rer. nat. Dr. -scient. med. Alexander Deutsch. Beide haben mir durch die hervorragende Betreuung neue Erkenntnisse in der Wissenschaft vermittelt. Mein Dank richtet sich auch an meine Kolleginnen Claudia Bodner und Sybille Hofer, die mir nicht nur mit Rat und Tat zur Seite standen sondern auch für die erforderliche Abwechslung sorgten. Bedanken möchte ich mich weiters bei Mag. Isabella Lassnig, die mir mit ihren ausgezeichneten Englischkenntnissen bei der Korrektur der Arbeit sehr geholfen hat. Dank gebührt auch meinen Freunden, die mich jederzeit moralisch unterstützten.

Abschließend gilt mein ganz besonderer Dank meiner Familie, ohne deren liebevolle Unterstützung ein Studium nicht möglich gewesen wäre.

I declare that I have authored this thesis independently, that I have not used other than the declared sources / resources and that I have explicitly marked all material which has been quoted either literally or by content from the used sources.

Ich erkläre an Eides statt, dass ich die vorliegende Arbeit selbstständig verfasst, andere als die angegebenen Quellen/Hilfsmittel nicht benutzt und die den benutzten Quellen wörtlich und inhaltlich entnommenen Stellen als solche kenntlich gemacht habe.

Contents

List of Figures

List of Tables

Nomenclature

C_P	Crossing point
C_T	Threshold cycle
ABC	Activated B-cell-like
ALL	Acute lymphoblastic leukemia
B-CLL	B-cell chronic lymphocytic leukemia
BAFF-R	B-cell-activating factor belonging to the TNF family receptor
BCR	B-cell receptor
Bp	Basepair
ddNTPs	Dideoxynucleotides
DLBCL	Diffuse large B-cell lymphoma
DNA	Deoxyribonucleic acid
DNMT	DNA methyltransferases
dNTPs	Deoxyribonucleotide triphosphate
DUB	Deubiquitinating enzyme domain
EC	Euchromatin
ES	Embryonic stem cells
EtBr	Ethidium bromide

Exo1	Exonuclease 1
FADD	FAS-associated death domain
FL	Follicular lymphoma
GCB	Germinal center B-cell-like
HC	Heterochromatin
HCL	Hairy cell leukemia
HDAC	Histone deacetylase
HKG	Housekeeping gene
HL	Hodgkin lymphoma
HMT	Histone methyltransferase
HSO_3-	Bisulfite
IκB	Inhibitor of NF-κB
Ig	Immunoglobulin
IL-1	Interleukin-1
LTbR	Lymphotoxin b receptor
MALT	Mucosa-associated lymphoid tissue lymphoma
MBD	Methyl-CpG binding domain
MBP	Methylcytosine binding protein
MCL	Mantle cell lymphoma
MSP	Methylation specific PCR
MZL	Marginal zone lymphoma
NF-κB	Nuclear factor kappaB transcription factor
NHL	Non-Hodgkin lymphoma

NK	Natural killer-cell
NTC	Non-template control
ORI	Origin of replication
OTU	Ovarian tumor
p.a.	pro analysis
PCR	Polymerase chain reaction
PMBL	Primary mediastinal B-cell lymphoma
RIP	Receptor interacting protein
RPPH1	Ribonuclease P RNA component H1
RRM	Ready reaction mix
RS	Richter syndrome
RT PCR	Real time polymerase chain reaction
SAP	Shrimp Alkaline Phosphatase
SWI/SNF	Switch/Sucrose Nonfermentable
TAQ	Thermus aquaticus
TDG	Thymine-DNA glycosylase
TERT	Telomerase reverse transcriptase
TLR	Toll-like receptor
TNF	Tumor necrosis factor
TNFAIP3	Tumor necrosis factor alpha-induced protein 3
TNFR1/2	Tumor necrosis factor type 1/2 receptor
TRADD	TNF-receptor-associated death domain
UNG	Uracil-DNA glycosylase

UTR	Untranslated Region
WM	Waldenström's macroglobulinemia

Abstract

Richter syndrome represents the transformation of chronic lymphatic leukemia (CLL) to an aggressive lymphoma, in the majority of cases in diffuse large B-cell lymphoma (DLBCL). Richter syndrome has a poor prognosis and the pathogenic mechanisms underlying transformation are poorly understood. The tumor suppressor gene TNFAIP3 (A20) is involved in the negative regulation of the NF-κB - pathway and has been shown to be inactivated in various lymphoid malignancies.

The A20 gene is encoded by a zinc finger protein containing a functional OTU domain at its N-terminal portion which hydrolyses polyubiquitin chains and seven zinc fingers at its C-terminal portion that show redundancy in inhibition of NF-κB activation. The aim of this study was to analyze whether TNFAIP3 is inactivated in Richter syndrome through genetic or epigenetic alterations.

Mutational analysis and promoter hypermethylation analysis of CpG islands showed that inactivation of A20 by mutation or epigenetic mechanisms seems to be of minor importance for the transformation to Richter syndrome. However, the gene copy number assay using real time PCR revealed 6/16 deletions (=37%) within the A20 locus. If confirmed by a complementary method these results indicate that deletions rather than mutations seems to be involved in the molecular pathogenesis of Richter syndrome and may represent a major contributor to lymphomagenesis in this lymphoma subtype.

Chapter 1

Introduction

1.1 Richter syndrome

Maurice N. Richter initially recognized 1928 the development of B-cell chronic lymphocytic leukemia (B-CLL) to a secondary large cell immunoblastic lymphoma [1] with a typical morphology reminiscent of diffuse large B-cell lymphoma (DL-BCL)). Therefore Richter syndrome represents the transformation of chronic lymphocytic leukaemia (CLL), the most common type of leukemia in Western countries, to an aggressive lymphoma, in majority of cases in DLBCL. RS most frequently involves the lymph nodes but extra-nodal localizations have also been reported [2].

1.1.1 Chronic lymphocytic leukaemia - CLL

Acute leukemias are blood cancers deriving from immature progenitor cells. A distinct subset of leukocytes are lymphocytes of the B-cell origin and CLL usually represents a malignant transformation of mature - partly antigen naive - B-cells. They originate in the bone marrow, differentiate in the lymph nodes and - after antigen binding by their B-cell receptor (BCR) - are capable of producing antibodies. However, transformed B-cells in CLL are not able to mount an efficient antibody response anymore. Thus, secondary antibody deficiency syndrome results in a profound immunosuppressive state with recurrent opportunistic infections. Because of their independency of growth signals CLL-cells proliferate uncontrolled and accumulate in the bone marrow and peripheral blood thereby displacing healthy unaffected blood cells.

1.1.2 Diffuse large B-cell lymphoma (DLBCL)

DLBCL represents a heterogeneous disease comprising several categories reflecting their distinct origin from different B cell differentiation states. Three molecular subtypes of this type of aggressive non-Hodgkin lymphoma are distinguished [3]:

- Activated B-cell-like (ABC) DLBCL: expression pattern of ABC DLBCL resembles that of cells committed to plasmacytic differentiation. Therefore ABC subtype DLBCL is thought to arise from postgerminal center B cells [3] [4].
- Germinal center B-cell-like (GCB) DLBCL: considered to derive from a GC centroblast [4].
- Primary mediastinal B-cell lymphoma (PMBL): considered to arise from thymic B-cells [5]

1.1.3 RS other than DLBCL

Over years several entities where included to the definition of RS such as the Hodgkin variant of Richter transformation [6], small noncleaved lymphoma, lymphoblastic lymphoma, and hairy cell leukemia (HCL) [7]. Mauro et al. observed transformation to Richter syndrome in 22 among 1011 B-CLL patients (18 cases DLBLC and 4 cases Hodgkin variant of RS) [8]. The frequency of RS is generally reported between 3-10% of patients with CLL but might be higher because postmortem examinations were not performed in most patients [9]. A very unusual variant of Richter syndrome is the development of a high-grade T-cell non-Hodgkin lymphoma from B-cell CLL [10].

1.1.4 Molecular pathogenesis of Richter syndrome

Even when restricting the definition of Richter syndrome exclusively to transformation of CLL to DLBCL, the clinical presentation of RS is heterogenous, including two biologically different conditions [2]:

- Transformation of chronic lymphocytic leukaemia cells to a clonally related DLBCL which applies to the majority of cases (80%) and
- development of DLBCL unrelated to the original CLL clone

Richter syndrome has a poor prognosis and the pathogenic mechanisms underlying transformation are poorly understood [11] [9]. Different genetic defects such as mutations of the tumor suppressor gene p53 [12] or p16(INK4A) [13], the loss of the cell cycle inhibitors p27 and p21, or decreased expression of the A-MYB gene [14] have been reported in B-CLL. Other recurring genes modified in RS are BCL11a/REL (2p16.1), MDM2 (12q15), BCL2(18q23), and TERT (5p15.33), but none of this lesions were identified in more than half of RS patients [11].

1.2 A20 / TNFAIP3

Three decades ago tumor necrosis factor (TNF) was identified as product of lymphocytes and macrophages that caused the lysis of certain types of tumor cells [15]. The best known member of this class is TNF- α that plays a key role in orchestrating the inflammatory response [16]. Deregulation of TNF production has been implicated in a variety of human diseases, including major depression [17], Alzheimer‘s disease [18] atherosclerosis, osteoporosis, autoimmune disorders, allograft rejection and cancer [15].

Tumor necrosis factor alpha-induced protein 3 (A20) is an inhibitor of NF-κB signalling (nuclear factor of kappa light polypeptide gene enhancer in B-cells, see chapter 1.2.1) and loss of this gene function plays an important role in lymphomagenesis suggesting that TNFAIP3 acts as a tumor suppressor gene [19].

1.2.1 NF-κB - pathway

Ranjan Sen et al. identified in 1986 NF-κB as a nuclear protein in cells that induce transcription of Ig light chain- genes that collaborate with a specific site in the κ Ig enhancer [20]. It quickly became evident that NF-κB is present in almost every cell type, bound to specific inhibitors (IκBs) which inactivate this nuclear factor. Several well characterized pathways inducing transcriptional activation are known but the nuclear factor pathway is particular in the rapidity of its activation and its unusual mechanism of regulation [21]. This pathway can be activated by many different stimuli such as cytokines (TNF), interleukin-1 (IL-1), growth factors, stress, viruses and bacteria [22]. Two different pathways for activating NF-κB exist: the classical and alternative NF-κB activation pathway.

On the basis of activation following to ligand binding of tumor necrosis factor type 1 receptor (=TNFR1, most effects of TNF are mediated by TNF-R1) the canonical (classical) NF-κB pathway is activated as shown in fig. 1.1. This pathway results in the increased transcription of target genes encoding chemokines, cytokines, and adhesion molecules, perpetuating inflammatory responses, and promoting cell survival. On the other side, the alternative pathway is induced by activation of certain TNF receptor family members, including lymphotoxin b receptor (LTbR), B-cell-activating factor belonging to the TNF family receptor (BAFF-R), CD40, and CD30. Activation of the alternative pathway controls the development of lymphoid organs and the adaptive immune system [23].

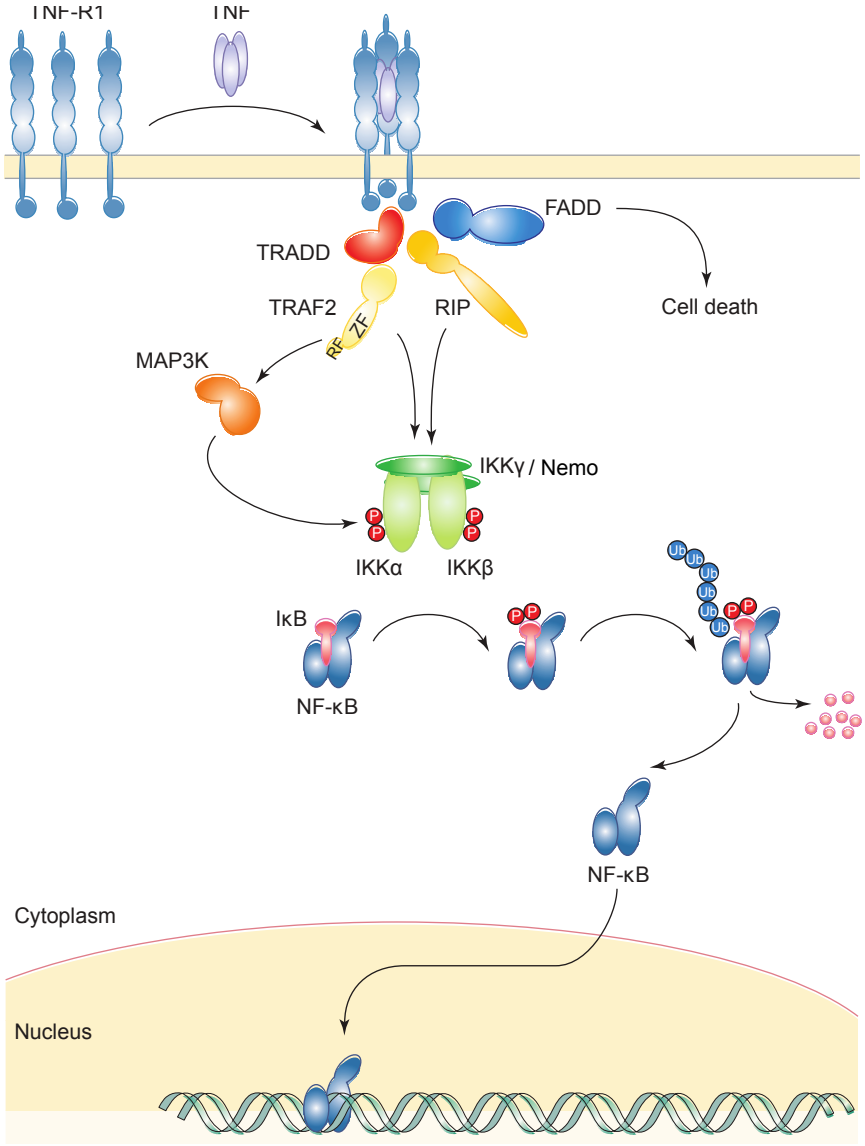

Figure 1.1: TNF mediated signaling to NF-κB via TNF-R1: Binding of TNF to TNF-R1 enables the receptor to recruit the cytoplasmic protein TNF-receptor-associated death domain (TRADD) which mobilizes a FAS-associated death domain (FADD), a receptor-interacting protein (RIP), and TNF-receptor associated factor 2 (TRAF2). RIP and TRAF2 contribute to the signalling pathway towards NF-κB activation via recruitment, phosphorylation and dimerization of IκB kinase (IKK) complex. The activated IKKs phosphorylate the inhibitory IκB protein which disassociates NF-κB in cytoplasm. Finally NF-κB binds to specific promoter sequences in the nucleus [22].

1.2.2 A20/TNFAIP3 gene

The A20 gene is localized on chromosome 6q23.3-q25 and is composed of 9 exons and 8 introns.

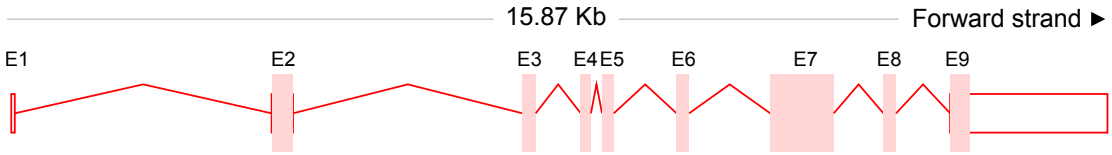

Figure 1.2: Gene structure: The A20 gene consists of 4,432 bps comprising 9 exons and translates to a protein with 790 amino-acid residues. Boxes represent exons, lines connecting the boxes introns. Filled boxes are coding sequence, and empty boxes are untranslated regions (UTR). Ensembl: Gene ID ENSG00000118503; Transcript ID ENST00000237289

The A20 gene is encoded by a zinc finger protein containing a functional OTU domain at its N-terminal portion which hydrolyses polyubiquitin chains [24] and seven zinc fingers at its C-terminal portion that show redundancy in inhibition of NF-κB activation [25].

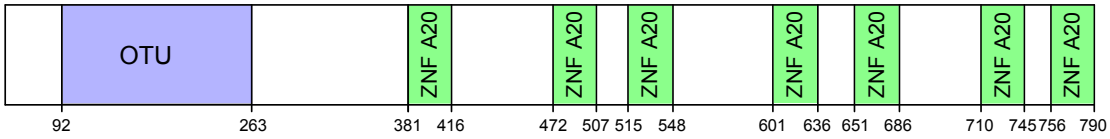

Figure 1.3: TNFAIP3 protein with characterized domains

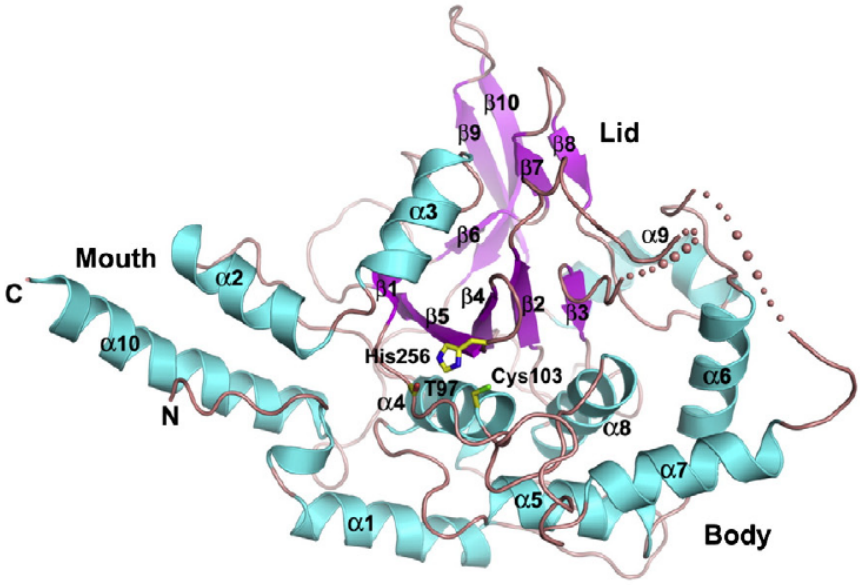

Figure 1.4: A20 Ribbon diagram: composed of 10 β-strands and 10 α helices, forming an anterior α-helical domain (mouth), a central β-sandwich domain (lid), and a posterior α-helical domain (body) [26]

1.2.3 A20 controls the NF-κB pathways

The OTU domain of A20, which contains a deubiquitinating enzyme (DUB) works together with the C-terminal domain, which is responsible for the ubiquitin ligase activity. RIP was identified as important target of A20 (see fig. 1.5). A20 is not only responsible for termination of TNF- induced signals, but also for the termination of Toll-like receptor-(TLR) induced activity of NF-κB by associating with TRAF6, a signalling molecule that regulates TLR signalling to NF-κB [27].

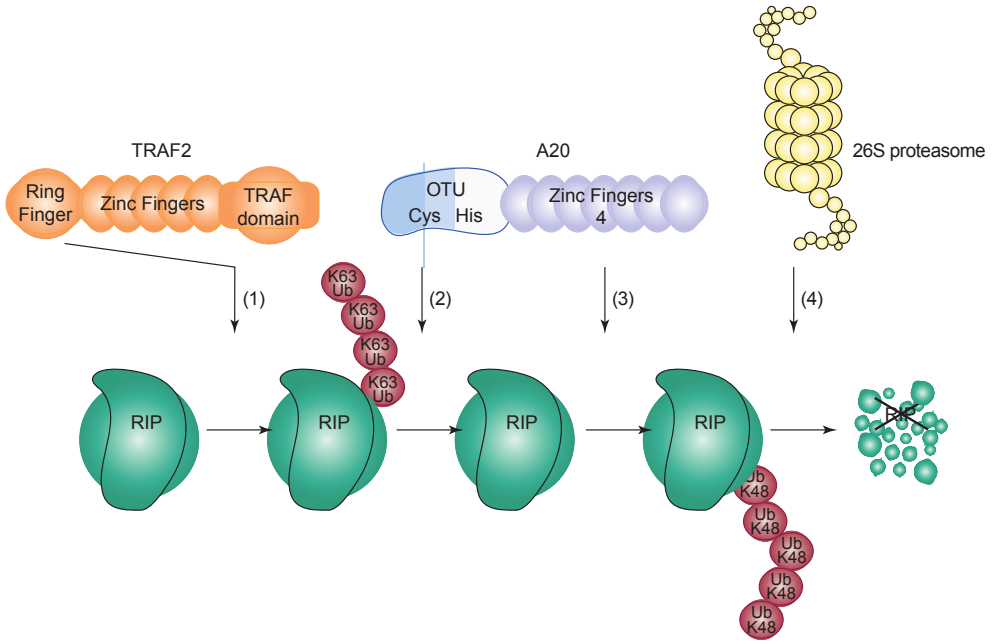

Figure 1.5: Negative regulation of NF-κB 1. Following ligand binding to TNF-R1, RIP becomes polyubiquitinated by the RING (Really Interesting New Gene) finger containing and RIP- interacting protein TRAF2 2. RIP becomes deubiquitinated by the OTU domain of A20 3. RIP is polyubiquitinated againby the fourth finger of C-terminal zinc finger domain of A20 4. Polyubiquitinating chains are linked via Lys48 so RIP1 is targeted for proteasome-mediated degradation. In consequence this leads to downregulation of IKK activity [22]

1.2.4 A20 inactivation in lymphoid malignancies

In many lymphoma entities a constitutive aberrant activation of NF-κB signaling was detected suggesting that A20 is involved in lymphomagenesis. Several studies showed genetical (mutations/deletion) and epigenetical (promoter methylation, see chapter 1.3.5) alterations, leading to A20 inactivation in Hodgkin lymphoma [28] [29] and non-Hodgkin's lymphomas like acute lymphoblastic leukemia (ALL) [30] [31], diffuse large B-cell lymphoma (DLBCL) [30] [31], follicular lymphoma (FL) [30] [31], mucosa-associated lymphoid tissue lymphoma (MALT) [32] [29] [31], mantle cell lymphoma (MCL) [30] [31], marginal zone lymphoma (MZL) [33], natural killer-cell lymphoma (NK) [31] and Waldenström's macroglobulinemia (WM) [34].

1.3 Genetics / Epigenetics

1.3.1 Deoxyribonucleic acid - DNA

This nucleic acid contains genetic information which is responsible for the development and proper function of all living organisms. X-ray structure analysis performed in the 1950s demonstrated the double-stranded nature of DNA, which ultimately resulted in the elucidation of the double helix structure in 1953 by James Watson and Francis Crick [35].

1.3.2 Structure of DNA

DNA usually exists of a double-stranded structure, with both strands combined to form the characteristic double-helix (Fig 3.3). Every single strand of DNA is a chain consisting of four different nucleotides: adenine, cytosine, guanine, and thymine bases. A base coupled with sugar is known as nucleoside, when added to a phosphate group, it is called nucleotide (Fig 1.6). 5´- position of the pentose cycle is coupled with the phosphate group with the 3´- position of the next pentose cycle [36].

Base	**Nucleoside**
Adenine	Adenosine
Guanine	Guanosine
Cytosine	Cytidine
Thymine	Thymidine

Table 1.1: Base - Nucleoside

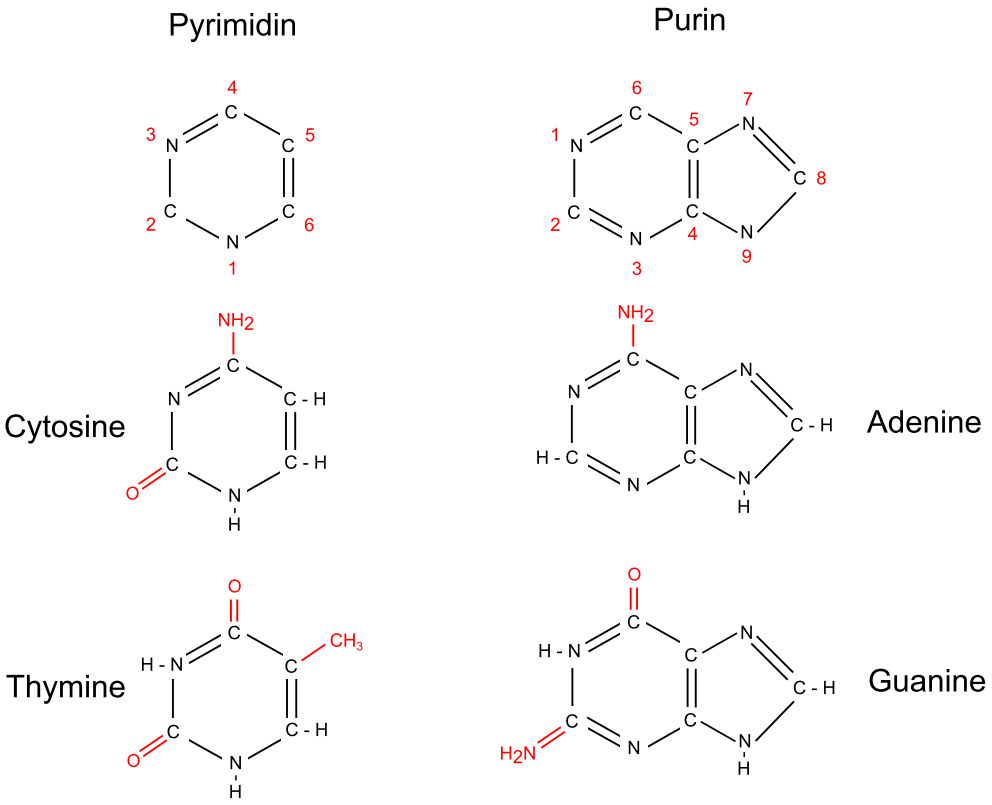

Figure 1.6: Purine and pyrimidine bases: Pyrimidine consists of four carbon- and two nitric atoms, both forming a ring. Purine includes two related hydrocarbon rings ranging from five to six links respectively.

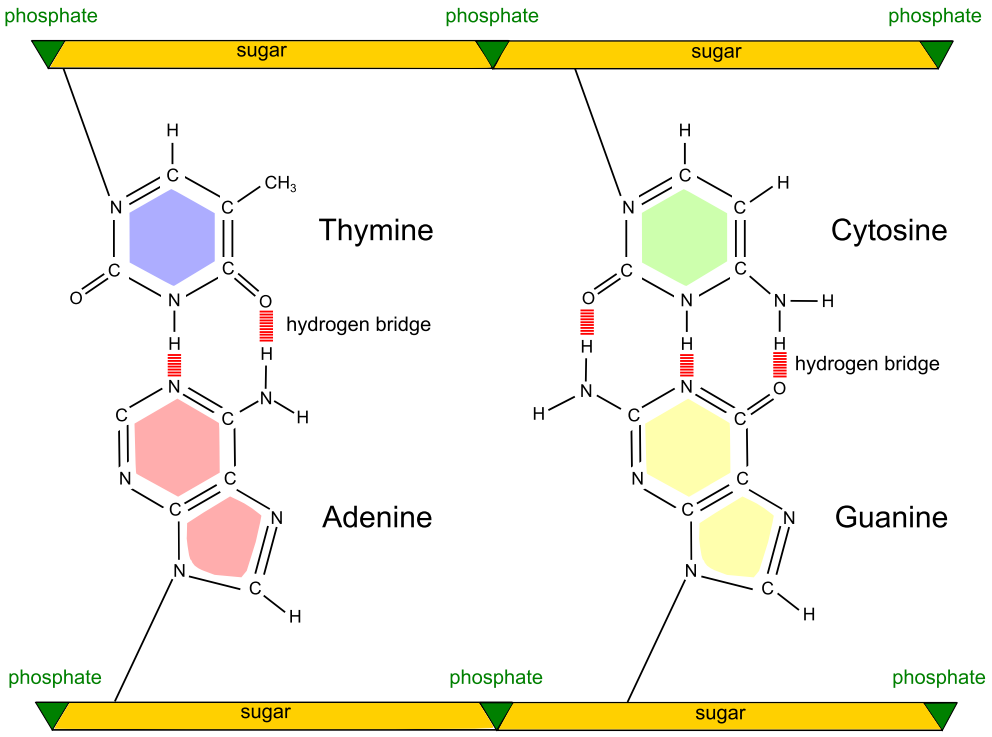

Figure 1.7: Chemical structure of DNA: Adenine and thymine are bound together by two hydrogen bridges, whereas cytosine and guanine are linked by three hydrogen bonds.

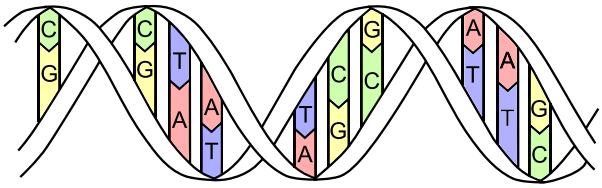

Figure 1.8: Characteristic double-stranded structure of DNA. Within DNA, purine constantly subtends a pyrimidine [35]. In this arrangement, each base pair is of similar width, thus holding the sugar-phosphate backbones an equal distance apart along the DNA molecule.

1.3.3 DNA replication

Through the mechanism of DNA replication, the whole genomic information of a cell is duplicated and propagated to daughter cells. DNA replication of both, prokaryotic and eukaryotic DNA starts at a unique sequence called the origin of replication (ORI), which serves as a specific binding site for proteins that initiate the replication process. The major initiation step is done by topoisomerases which unwind the DNA strands. Additional proteins including helicase and single-stranded DNA-binding proteins then act to continue unwinding and exposing the template DNA, and primase initiates the synthesis of the leading strands [37]. Two replication forks are formed and move in opposite directions along the chromosome (fig. 1.9). Finally DNA Polymerase extends the leading strand in one continuous motion and the lagging strand in a discontinuous motion (due to the Okazaki fragments)

In contrast to prokaryotes, eukaryotes initiate replication at multiple origins.

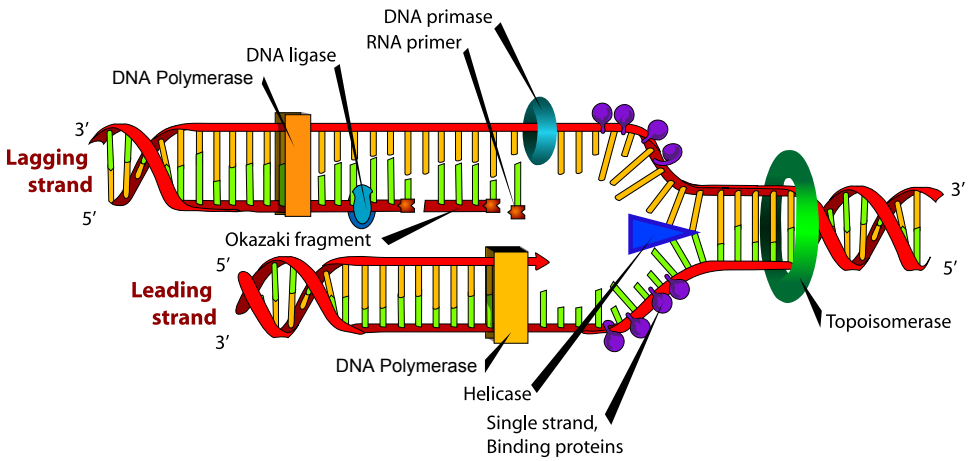

Figure 1.9: **Steps of DNA replication: 1. Initiation and unwinding:** Breaking of hydrogen bonds between bases of the two antiparallel strands by helicase. The initiation point where the splitting starts is called "origin of replication". The structure that is created is known as replication fork. **2. Primer synthesis:** Binding of RNA primase at the the initiation point of the 3'-5' parent chain. RNA nucleotides are the primers for the binding of DNA nucleotides. **3. Elongation:** The addition of nucleotides to the new DNA strand, DNA is always synthesized in the 5'-to-3' direction. **4. Termination:** This process happens when the DNA Polymerase reaches to the end of the strands.

1.3.4 Chromatin

The combination of DNA, RNA with associated proteins is called chromatin, representing an obligatory content of all cell nuclei. Depending on the stage of the cell cycle and cell function, chromatin is variably dense packed representing 2 different functional states with an open chromatin structure (euchromatin) enabling DNA transcription and a dense chromatin state (heterochromatin) representing lack of transcriptional active areas. Correct and secure DNA packaging is important for DNA replication as well as repair and recombination. The principle composition of chromatin is identical in all eukaryotes. Nucleosomes are subunits of chromatin consisting of a short DNA and a core of histone proteins.

1.3.5 Methylation

DNA methylation is an epigenetic modification that is involved in various cell- processes such as differentiation and proliferation [38], transcriptional regulation [39], genomic imprinting [40], X-chromosome inactivation [41], silencing of repetitive elements, maintenance of genomic stability [42] and DNA repair [38]. Transcriptional silencing of tumor suppressor genes, associated with DNA methylation, is a common epigenetic event in hematologic malignancies [43]. Epigenetic modification results in heritable changes in DNA structure without altering the sequence. As far as DNA methylation is concerned, a methyl group is attached to the 5 position of the cytosine pyrimidine ring [44]. This process is mediated by DNA methyltransferases (DNMT1,3a and 3b).

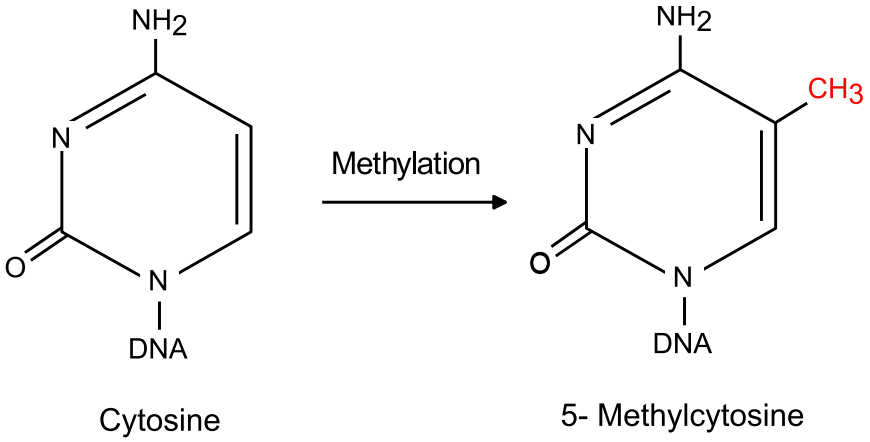

Figure 1.10: Conversion from cytosine to 5-methylcytosine by attaching a methyl group

1.3.6 DNA methyltransferases - DNMT

1.3.6.1 DNMT1

DNA methyltransferase 1 initiates the transfer of a methyl group from S-adenosylmethionine to the 5 position of the cytosine pyrimidine ring [44]. DNMT1 methylates hemimethylated dinucleotides in mammals and is the major maintenance methyltransferase (Fig. 1.11). This methyltransferase also mediates alterations in gene expression during development. Overexpression of DNMT1 induces de novo methylation in fibroblasts and myocytes [44].

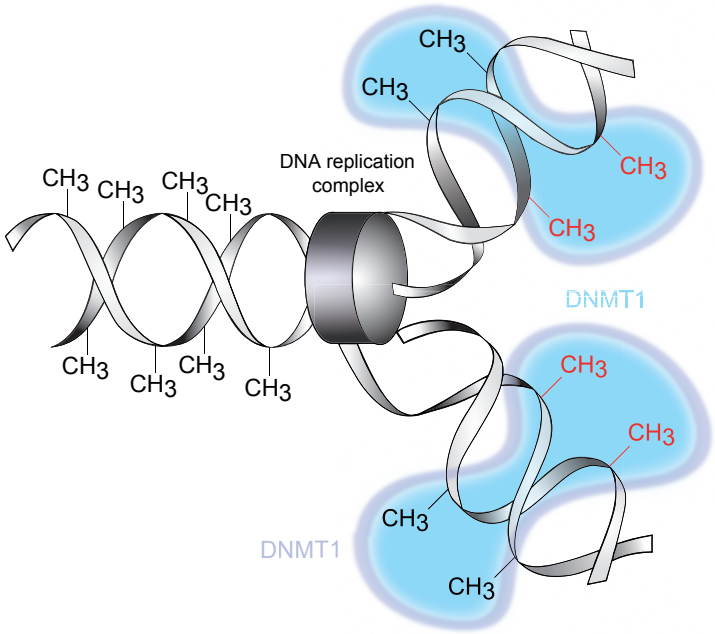

Figure 1.11: DNA methyltransferase 1: The enzyme encoded by DNMT1 transfers methyl groups to cytosine in hemimethylated CpG sites after DNA replication by reading the methylation pattern of the parental strand

Recent work identified DNMT2, which contains all characteristics of DNA methyltransferases but demonstrated no detectable methyltransferase activity in vitro [45].

1.3.6.2 DNMT3a / DNMT3b

Two new methyltransferases were discovered (DNMT3a, DNMT3b) recently [46]. DNMT3a and DNMT3b are encoded by two distinct genes and are widely expressed in undifferentiated ES cells. After terminating differentiation these proteins are downregulated. Their functions largely overlap and both are mainly responsible for *de novo* methylation during development [47].

1.3.7 CpG islands

CpG islands are areas, containing increased density of the dinucleotide sequence cytosine and guanine, with "p" simply indicating the connection of cytosine and guanine by a phosphate diester bond. Methylation of CpG sites within the promoter region of genes generally leads to gene silencing, a feature found in a number of human cancers (i.e. silencing of tumor

suppressor genes). In contrast, the hypomethylation of CpG sites has been associated with the overexpression of oncogenes within cancer cells.

The typical occurrence of guanine and cytosine in human genome is about 40% hence the computed value of CG dinucleotides approximates 4%. However the real occurrence of CpG in humans is at much lower frequency (0.8%). This effect is called CG suppression or depletion and relates to the tendency of 5-methylcytosine which are spontaneously deaminated to thymidine, whereas unmethylated cytosine deaminates to uracil [48]. These defects can be compensated by thymine-DNA/ uracil-DNA glycosylases. Deamination to uracil is immediately restored by the DNA glycosylases uracil-DNA glycosylase (UNG), single-strand selective monofunctional uracil DNA glycosylase (SMUG1), methyl-CpG binding domain 4 (MBD4) and thymine-DNA glycosylase (TDG) [49]. CpG islands are characterized by CpG dinucleotide content of at least 60% whereas the occurrence of CpG dinucleotide ranges between 6-8% [48]. They generally appear near the transcription site of genes.

DNA methylation typically occurs in a CG dinucleotide context. Previous studies proved that the fraction of methylation depends on the origin of the DNA. Nearly 1.00 mole percent 5-methylcytosine were traced in those DNA-types originating in thymus and brain. In comparison, merely 0.76 and 0.84 mole percent 5-methylcytosine turned up in placental and sperm DNA [50].

1.3.8 DNA-Methylation and gene expression

DNA methylation plays an important role in gene expression in eukaryotes. It is assumed that DNA-methylation inhibits gene expression. There are two general ways/mechanisms for methylation to prevent gene transcription: In general the transcription factor binds to specific DNA sequences in unmethylated cases.

1. Methylation can inhibit this process directly by interrupting the binding process of a specific DNA binding factor to its recognition site. (Fig. 1.12) [51]

2. Furthermore proteins have been reported which specifically bind to methylcytosine and are able to repress transcription.

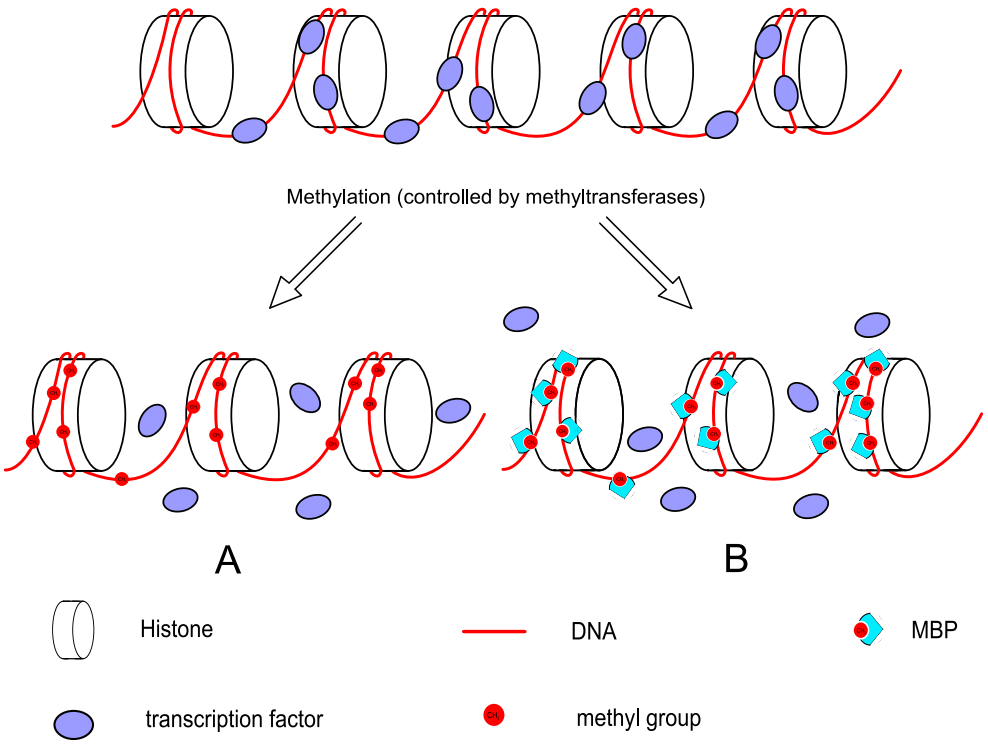

Figure 1.12: Methylation inhibits the binding of transcription factor: While transcription factor binds to specific DNA sequences in unmethylated DNA, transcription factor binding is inhibited by methylation (A) Further MBPs bound specifically to methylated CpGs also avoid access of transcription factors to their binding site (B)

1.3.8.1 Methylcytosine binding protein (MeCP) and Methyl-CpG binding domain (MBD)

Human proteins MeCP1, MeCP2, MBD1, MBD2, MBD3, and MBD4 comprise a family of nuclear proteins related by the presence in each of a methyl-CpG binding domain (MBD). Each of these proteins, with the exception of MBD3, is capable of binding specifically to methylated DNA thereby influencing transcription. They bind to a variety of methylated sequences, and mediate repression of gene expression.

MeCP1 and MeCP2: Both are mammalian proteins which able to inhibit transcription depending on methylation. MeCP2 is the most prominent of the methylcytosine binding proteins and contains a transcriptional repression domain suggesting that MeCP2 may play a role in the formation of inert chromatin [52].

Methyl-CpG binding domain (MBD) 1-4: MBD1, MBD2, and MBD4 are capable of binding to DNA that contains one or more symmetrically methylated CpGs. MBD1, and MBD2 can also repress transcription from methylated gene promoters. The methyl CpG binding domain of human MBD3 may not directly bind to methylated CpG sites but does interact with HDAC1 and plays a role in histone deacetylation and nucleosome remodeling. MBD4 functions as a G/T mismatch glycosylase [44].
MeCP2 in particular interacts with various sets of proteins: [53]

- Histone deacetylase (HDAC): an enzyme that removes acetyl groups from the amino acid lysine on a histone. Based on this process, lysin is charged positive and increases the affinity to the negative charged DNA phosphate frame, resulting in a more compact chromatin structure.
- Protein Sin3A: acts as a transcriptional repressor.
- Histone methyltransferase (HMT): catalyzes the transfer of methylgroups to arginine and lysine residues. This process increases chromatin condensation.
- Switch/Sucrose Nonfermentable (SWI/SNF): SWI/SNF complex is capable of altering the position of nucleosomes along DNA and is involved in nucleosome remodeling.

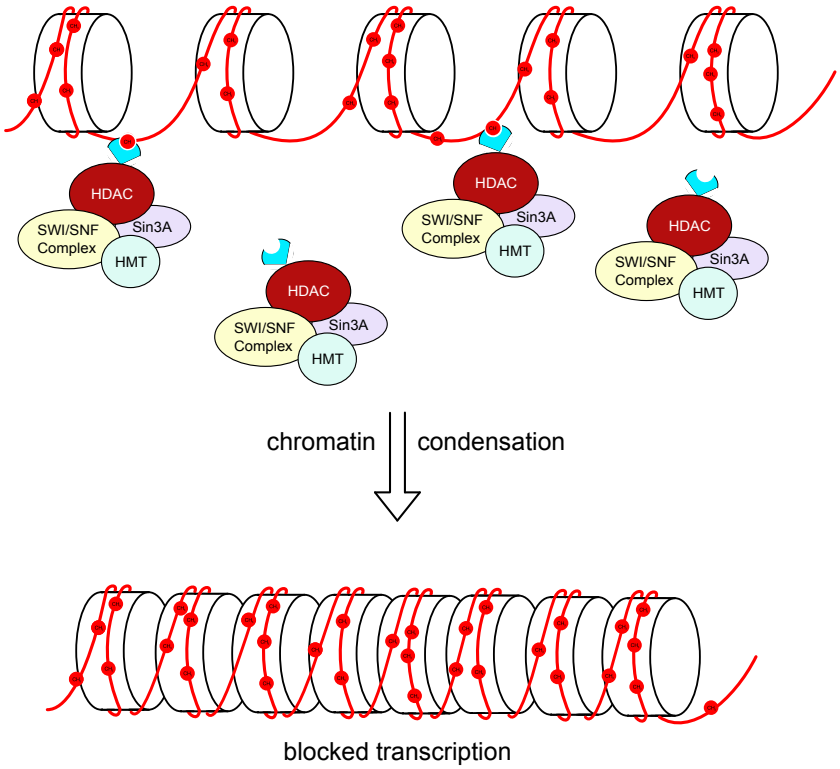

Figure 1.13: Blockade of transcription by methylcytosine binding domain (MBD) mediated binding of MeCP to methylcytosine. A complex of HDAC, HMT, SWI/SNF and Sin3a can bind to this MBP and effectuates histone modification (chapter 1.3.8.2)

1.3.8.2 Histone modification and chromatin function

Histones are proteins located in eukaryotic cell nuclei where chromosomal DNA coils up and forms a structural unit with a higher organization-level, the so-called nucleosomes. Nonhistone proteins together with nucleosomes constitute chromatin, organized in two different structures: heterochromatin and euchromatin.

- **Heterochromatin** (HC) is the most condensed form of chromatin and can be divided in facultative and constitutive HC. Constitutive HC - due to its packing density - represents a permanent state of transcriptional inactivity where RNA polymerase and other proteins involved in transcription are denied access. Facultative HC is often the result of histone methylation. Constitutive and facultative heterochromatin are both silent, with only facultative HC being able to interchange between heterochromatin and euchromatin (Fig. 1.13) [54].

- **Euchromatin** (EC) is an open and usually active form of chromatin allowing direct DNA transcription.

1.3.9 Tumor suppressor gene methylation

Tumor suppressor genes have a controlling function in cell cycle and apoptosis. They have a negative effect on cell cycle regulation or promote apoptosis. This property protects cells from undergoing malignant transformation. They also protect the genome from mutagenic events and prevent metastasis and cellular migration [43]. Promoter hypermethylation (hypermethylation of CpG islands increases the epigenetic methylation of cytosine residues in the promoter) represents a distinct mechanism of tumor suppressor gene inactivation and is equivalent in its function to an inactivated tumor suppressor gene. It is an important and well recognized mechanism in oncogenesis of many tumor types [55] [43]. Thus screening methylation patterns in CpG islands is essential for physiological/normal and pathologic gene expression.

Chapter 2

Objectives

Richter syndrome represents the transformation of chronic lymphatic leukemia (CLL) to an aggressive lymphoma, in majority of cases in diffuse large B-cell lymphoma (DLBCL). Richter syndrome has a poor prognosis and the pathogenic mechanisms underlying transformation are poorly understood. The tumor suppressor gene TNFAIP3 (A20) is involved in the negative regulation of the NF-κB - pathway and has been shown to be inactivated in various lymphoid malignancies.

The A20 gene is encoded by a zinc finger protein containing a functional OTU domain at its N-terminal portion which hydrolyses polyubiquitin chains and seven zinc fingers at its C-terminal portion that show redundancy in inhibition of NF-κB activation.

The aim of this study was to analyze whether TNFAIP3 is inactivated in Richter syndrome through genetic (mutations and/or deletions) or epigenetic (promotor methylation) mechanisms.

Chapter 3

Materials

3.1 Specimens

Lymphoma entities were classified according to the WHO classification of lymphoid neoplasms. Macrodissected tissue containing >80% lymphoma cells from fresh frozen tissue was processed for DNA isolation. Direct sequencing of A20 was performed on 9 DLBCL (3 GCB, 6 NGCB) and on 16 Richter samples. To investigate whether genomic deletion may affect Richter syndrome development, 16 RS samples were used to determine frequencies of A20 deletion. Because inactivation mechanisms other than mutation or deletion may affect RS development, promotor methylation status was checked of all RS.

3.2 Glass flasks and plastic

Pipets, multistep pipets, multichannel pipets, 1,5 ml tubes, pipet tips (ep Dualfilter) were bought from Eppendorf (Hamburg, Germany). 15/30 ml falcon tubes were purchased form BD Labware (Franklin Lakes; USA). 500 ml glass flasks and beakers were bought from Brand (Wertheim, Germany).

3.3 Chemicals / reagents

Chemicals were used with the degree of purity "pro analysis" (p.a.) and were bought from Applied Biosystems(Foster City, USA), Biozym (Oldendorf, Germany), Merck (Darmstadt, Germany), Invitrogen (Lover, Austria), Fermentas Life Sciences (St. Leon-Rot, Germany),

Millipore (Temecula, California) Pequlab (Erlangen, Germany), Qiagen GmbH (Hilden, Germany) and Sigma-Aldrich Chemie GmbH (Steinheim, Germany).

3.3.1 Buffers and solutions

Biozym ME Agarose, *CpGenome*^{TM} Universal Methylated DNA (Millipore), *CpGenome*^{TM} Universal Unmethylated DNA (Millipore), 50x TAE buffer (Merck), 10x PCR buffer (Qiagen), Proteinase K (Sigma)

3.3.2 Standards

For gel electrophoresis following Standards were used:

- *GeneRuler*^{TM} 1 kb Plus DNA Ladder (0.1µg/µl; Fermentas)
- *GeneRuler*^{TM} 100 bp Plus DNA Ladder (0.1µg/µl; Fermentas)
- *GeneRuler*^{TM} 50 bp DNA Ladder (0.1µg/µl; Fermentas)

3.4 Commercial kits

Following commercial kits were used for amplification, DNA extraction, purification and sequencing:
Bisulfite treatment: *MethylCode*^{TM} Bisulfite Conversion Kit
DNA amplification: HotStar Taq Polymerase Kit (Qiagen)
DNA clean up: *SigmaSpin*^{TM} 96-Well Post-Reaction Clean-Up Plates (Sigma-Aldrich Chemie GmbH)
DNA extraction: QIAamp DNA Mini Kit
DNA purification: SAP/ ExoI (Fermentas Life Science GmbH)
DNA sequencing: BigDye Terminator v1.1 Cycle Sequencing Kit (Applied Biosystems)
Real time PCR: EXPRESS One-Step *SYBRGreenER*^{TM} SuperMix Kit (Invitrogen Life technologies)

3.5 Equipment

Centrifuge: Heraeus "Biofuge fresco" (Osterode; Germany); Heraeus Multifuge 3 L-R
Applied Biosystems 2720 Thermal Cycler
Bio-Rad iCycler Thermal Cycler
Bio-Rad Thermal Cycler MyCycler TM Serial No 580BR 1448
Electrophoresis power supply: Bio-Rad PowerPac Basic TM 300V 7400mA / 75W
Incubator and Heating block: Eppendorf "Thermomixer comfort" (Hamburg; Germany)
Migration chamber: Bio-Rad SUB-CELL ®GT
Nanodrop: Eppendorf BioPhotometer
Photosystem: Molecular Imager Gel Doc TM EQ system
Real-time PCR system: GeneAmp ®5700 Sequence Detector (Applied Biosystems; Foster City; CA)
Scale: Sartorius GP3202-OCE
Sequencer: Applied Biosystems Hitachi 3730 DNA Analyzer
Shaker: Peqlab "Centrifuge/Vortex Combi-Spin FVL-2400"
UV-Lamp: Bio-Rad UV Transilluminator 2000
Vortexer: Yellow line (North Carolina; USA)

3.6 Primer

All Primers were bought from Eurofins MWG Operon (Ebersberg; Germany).

3.6.1 Primer for Sanger sequencing

Primer	Primer sequence
Exon 2 forward	5' CCGGGAGTAGAGGTGCTA 3'
Exon 2 reverse	5' GTCTGCTATTATCACATACCCC 3'
Exon 3 forward	5' TCAGTTTGCCCTTGACTAGGA 3'
Exon 3 reverse	5' TGAGTCCCACTGGAGGTTTC 3'
Exon 4 forward	5' GGGAGTACAGGATACATT 3'
Exon 4 reverse	5' GCTGGAAAGCATTTAAGTA 3'
Exon 5 forward	5' ACCTAAGGGCCTCATTTTCC 3'
Exon 5 reverse	5' AGCAAAAAGGAAAACCGTGA 3'
Exon 6 forward	5' TGAGATCTACTTACCTATGGCCTTG 3'
Exon 6 reverse	5' AGGGTGGCAGCAACTCAG 3'
Exon 7 forward	5' GCTAATGATGTAAAATCTTGTGTGTG 3'
Exon 7 reverse	5' CAGGAACAAAACCCCTTCTG 3'
Exon 8 forward	5' CTCTGTATCGGTGGGGTGAC 3'
Exon 8 reverse	5' CAAAAAGCATCGAACACACG 3'
Exon 9 forward	5' GCTTGGCGGTTTTCCTCAG 3'
Exon 9 reverse	5' CTTTGCTTTCTAAGGCCACCT 3'

3.6.2 Primer for real time PCR

Primer	Primer sequence
A20Ex4-72F	5' TCAGTACAACTCACTGGAAGAAATACAC 3'
A20Ex4-122R	5' AGGATGTTGCAAAGGACAAATATG 3'
A20Ex6-2F	5' AATCCGAGCTGTTCCACTTGTT 3'
A20Ex6-52R	5' AAGTCTTCAAATCTTCCCCGGT 3'
TERT Exon2-1273F	5' GGGAAGCATGCCAAGCTCT 3'
TERT Exon2-1323R	5' CACGCTCATCTTCCACGTCA 3'
RPPH1-225F	5' CTTTGCCGGAGCTTGGAAC 3'
RPPH1-275R	5' GCCATTGAACTCACTTCGCTG 3'

3.6.3 Primer for methylation specific PCR

Primer	Primer sequence
Primer 1 forward methylation	5' TTTTCGGAGAGGTAATCGTC 3'
Primer 1 reverse methylation	5' AACGCCAAATAAACGATACC 3'
Primer 1 forward no methylation	5' GTTTTTTGGAGAGGTAATTGTT 3'
Primer 1 reverse no methylation	5' CCAACACCAAATAAACAATACC 3'
Primer 2 forward methylation	5' TTGGCGTTTTGTTTTTTTC 3'
Primer 2 reverse methylation	5' CGTCGAACTAATCCTACACAA 3'
Primer 2 forward no methylation	5' GTTGGTGTTTTGTTTTTTTT 3'
Primer 2 reverse no methylation	5' CCATCAAACTAATCCTACACAA 3'

Chapter 4

Methods

4.1 DNA extraction

A test run using two samples (R24H and R17L) comparing the classical phenol-chloroform extraction (DNA extraction protocol from frozen tissue sections http://waldman.ucsf.edu/Protocols/dna.frozen.htm) with extraction using DNA mini kit (Qiagen), demonstrated an outcome in favor of the DNA mini kit (see fig. 4.1). . Later the amount of DNA concentration was determined thanks to Nanodrop BioPhotometer technique (Eppendorf).

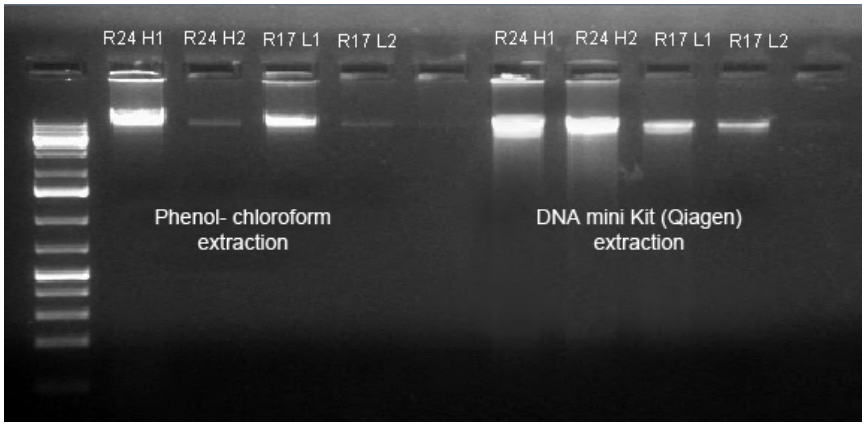

Figure 4.1: Comparison of DNA extraction: Phenol-chloroform vs DNA mini kit (Qiagen) Phenol-chloroform extraction: R24 H1 184ng/µl first dilution step, R24 H2 3ng/µl second dilution step, R17 L1 30ng/µl first dilution step, R17 L2 1ng/µl second dilution step, DNA mini Kit extraction: R24 H1 78ng/µl first elution step, R24 H2 65ng/µl second elution step, R17 L1 23ng/µl first elution step, R17 L2 18ng/µl second elution step

4.2 Mutational analysis: Sanger sequencing

DNA sequencing means detecting the order of the nucleotide bases adenine, thymine, cytosine and guanine. First step is to amplify DNA with PCR.

4.2.1 Polymerase chain reaction - PCR

With this technique it is possible to amplify a few copies of DNA exponentially according to the numbers of repeating cycles (Fig 4.2).

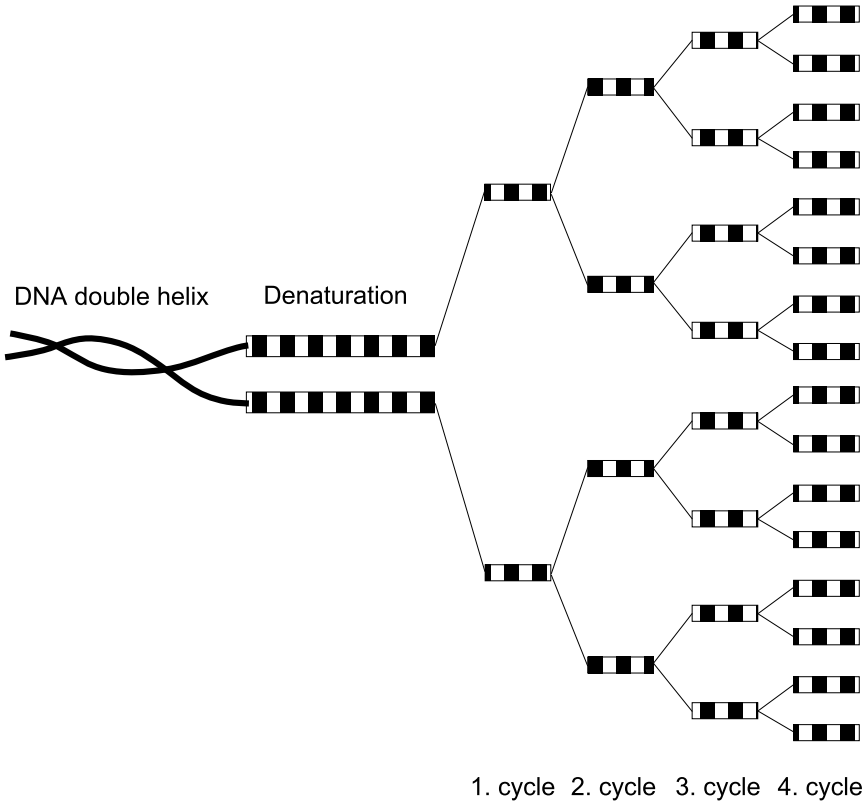

Figure 4.2: Exponential amplification of polymerase chain reaction. The number of DNA strands doubles with each successive cycle (in case of 100% efficiency)

The first step of PCR simply is about mingling template DNA with two appropriate oligonucleotide primers (see chapter 3.6.1) The latter flank the DNA segment to be amplified, deoxyribonucleoside triphosphates (dNTPs), buffer, and a thermostable DNA polymerase

PCR protocol	
Aqua dest.	29 µl
10x PCR Buffer	4 µl
Primer forward (100pmol)	1.5 µl
Primer reverse (100pmol)	1.5 µl
dNTPs (10mM)	0.8µl
TAQ Polymerase	0.2 µl
Template	3 µl
Total Volume.	40 µl

Table 4.1: PCR protocol for 3 µl DNA

extending the annealed primers. The amplification-process was assisted by QIAGEN HotStar TAQ polymerase kit. TAQ is termed Thermus aquaticus DNA polymerase purified from the thermophilic bacterium, which is resistant to incubation as up to 95 °C. This fast polymerase increases specification, yield, sensitivity, and length of targets subject to amplification [56] [57].

Comprehensive testing approved the mixing ratio of table 4.1.

Cycles of repeated heating and cooling of the reaction amplify DNA (Fig 4.3). Figure 4.4 shows PCR program for amplification of A20 gene. To check success of PCR gel electrophoresis was made afterwards.

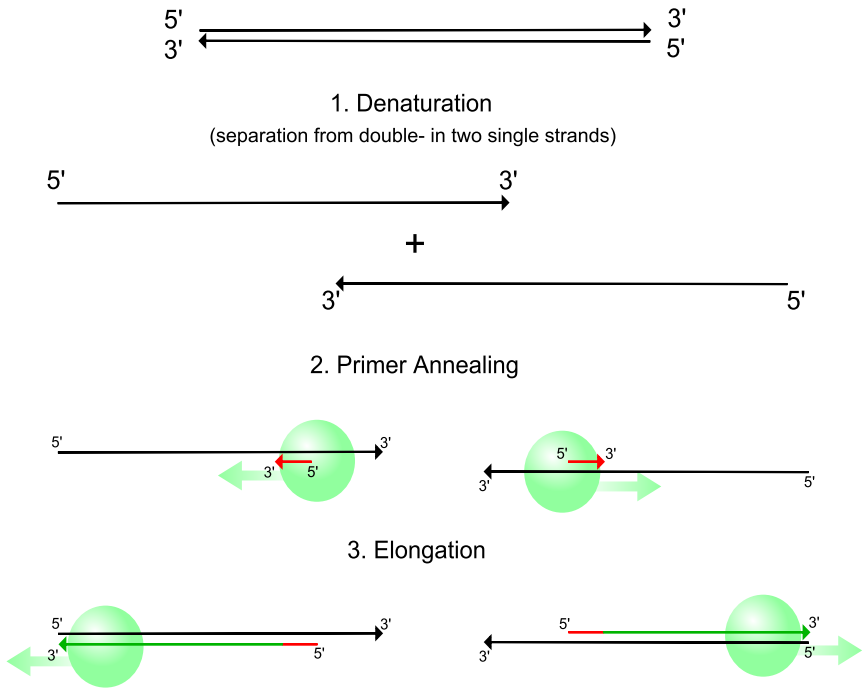

Figure 4.3: Schematic drawing of PCR cycle: 1. Denaturation: the reaction mixture is heated to separate complementary DNA strands 2. Primer annealing: the mixture is cooled to allow annealing of synthetic primers with complementary nucleotide sequences effecting every single end of DNA 3. Elongation: temperature is repeatedly raised, allowing DNA polymerase to synthesize new DNA strands by nucleotide bases being added to the primers.

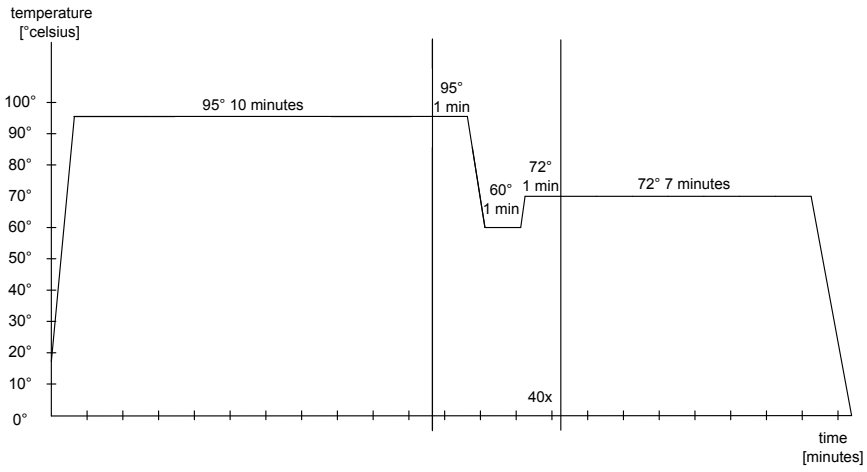

Figure 4.4: PCR program for A20 amplification: 95° DNA denaturation, 60° Primer annealing, 72° extension

4.2.2 Agarose gel electrophoresis

Agarose gel electrophoresis is a method to separate a mixture of DNA fragments by length. To achieve that, the DNA mixture was filled into one end of an agarose gel matrix. After applying an electric field, the fragments were moved to the positive electrode (due to a negative- charged DNA). The movement of DNA molecules by the gel matrix depends on size. A blue loading dye (Fermentas), also migrated to the positive pole is added to the samples to track the progress in the gel. After PCR, millions of terminated and equally sized molecules size came about, each migrating to the same place and "band" in the gel.

1% agarose gels were freshly prepared. Therefore 1.5 g agarose was mixed with 150 ml 1x TAE buffer. After being heated and not prior to complete melting, 3 µl ethidium bromide (EtBr, used to make bands visible under UV-light excitation) were added to 150 ml agarose gel. After solidifying 10 µl DNA samples and 2 µl loading dye were assigned for electrophoresis. Then 5 µl of 1 kb Plus DNA Ladder was applied. The remaining 30 µl could be subsequently processed for Sanger sequencing. Finally, with the help of exoSAP, a PCR was cleaned up.

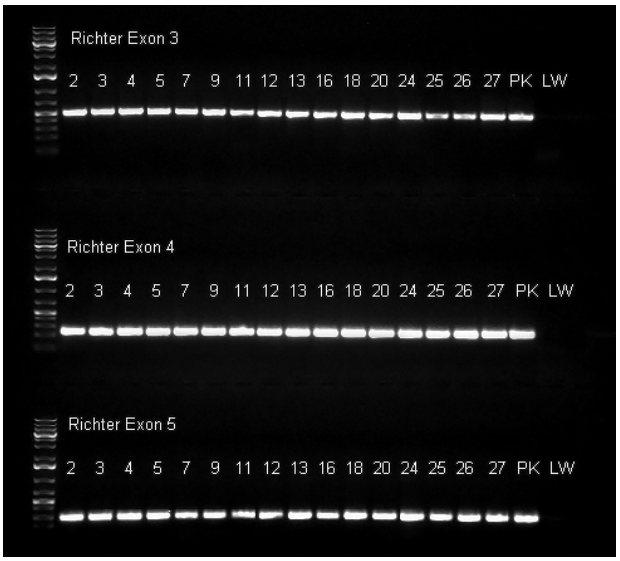

Figure 4.5: Agarose gel electrophoresis: 1 kb Plus ladder (Fermentas), Exon 3-5, Richter samples 2-27, PK = positive control, LW = negative control (contains no DNA)

4.2.3 ExoSAP

ExoSAP removes remaining primers and unconsumed dNTPs form PCR in order to eliminate any influence likely to effect DNA sequencing. For this procedure, 3 µl shrimp alkaline phosphatase SAP (removes phosphate monoester of the unbound dNTPs [58]), 1,35 µl aqua dest. and 0,15 µl exonuclease 1 (digest unbound primers) were added to each sample. After mixing, the sample was incubated at 37 °C for 30 minutes. As a result, exonuclease degraded single stranded DNA into free dNTPs and SAP inactivated free dNTPs by removing the phosphate groups. Finally the sample was heated at 75 °C for 15 minutes to inactivate ExoSAP.

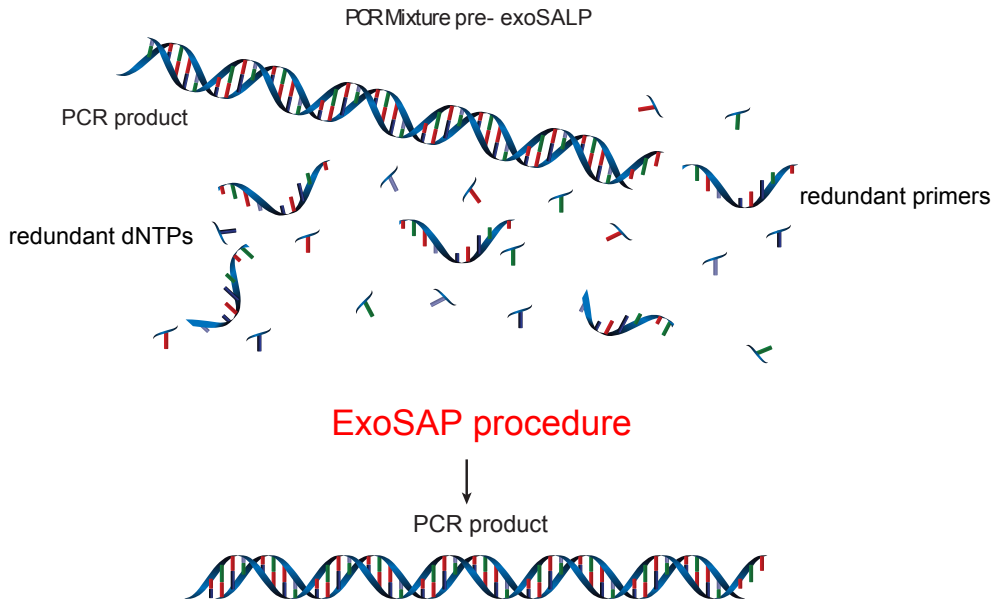

Figure 4.6: ExoSAP: After PCR many undesirable residues (remaining primers, unconsumed dNTPs) were found in mixture. After ExoSAP pure PCR product persisted

This purified product proved to be essential for the achievement of sequencing PCR.

4.2.4 Cycle sequencing PCR

Cycle sequencing uses thermostable DNA polymerase and dideoxynucleotide triphosphates (ddNTPs) to generate chain-termination sequence with a temperature-cycling format serving as a tool. ddNTPs do form an analogy to the natural 2´-dNTPs but also lack the 3´-

Cycle sequencing protocol	
RRM	4 µl
Primer	1 µl
Sequencing buffer	4 µl
Aqua dest.	7 µl
Template.	4 µl
Total Volume.	20 µl

Table 4.2: Cycle sequencing protocol: forward and reverse primer are separate approaches in different tubes

hydroxyl group [59] which is vital for the chain to be extended. Termination itself occurs after ddNTP is incorporated [60]. There are two fundamental differences between an usual PCR amplification and a cycle sequencing PCR: The former only uses one primer during the cycle-sequencing reaction, which applies to prime synthesis of one DNA-strand. Another difference lies in the presence of ddNTPs, more acurately each sequencing reactions creating the essential base-specific terminations. The result is a linear amplification of the sequenced product, leading to an increase of the signal generated while a sequencing reaction was under way [61].

After comprehensive testing, reagents listed in table 4.2 were added for each reaction to a separate tube and taken to the cycler (program see fig 4.7).

4.2.5 Sequencing Reaction Clean-Up

For this procedure $SigmaSpin^{TM}$ post-reaction clean-up plates respectively columns were used. They remove excluded dyes, excess salts, and other interfering reaction components.

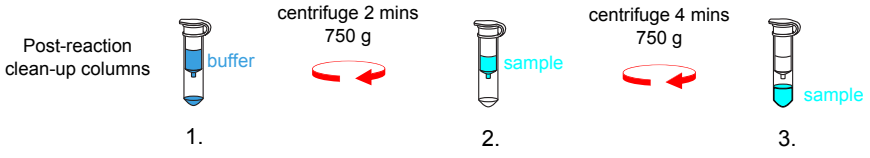

Figure 4.8: Sequencing reaction clean-up: 1. First centrifugation (750g 2 minutes) removes the buffer which is discarded afterwards 2. Samples can be loaded and the columns are centrifuged a second time (750g 4 minutes) 3. Finally the spin column contains the purified sample

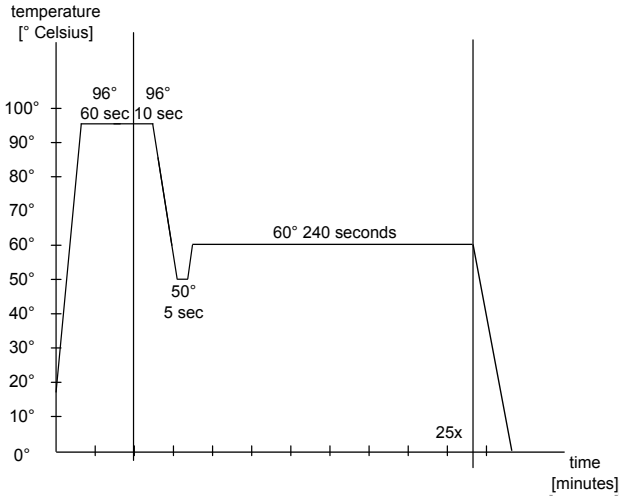

Figure 4.7: PCR program for cycle sequencing reaction: 96° DNA denaturation, 50° Primer annealing, 60° extension

4.2.6 Sanger Sequencing

The Sanger method combines synthesis of a complementary DNA template using 2´-deoxynucleotides (dNTPs) and the inhibitory activity of 2´,3´-dideoxynucleotides (ddNTPs) on DNA polymerase I. A new DNA strand is synthesized using an existing strand as template (see chapter 1.3.3). The 5´carbon of a deoxynucleotide is joined with the 3´carbon at the end of the chain, exactly where hydroxyl groups form ester linkages with a central phosphate.

Sanger incubated a short primer as well as a template with DNA polymerase, the latter being combined with both dideoxythymidine triphospate and deoxythymidine triphospate (one radioactively labeled with ^{32}P). He obtained collections of DNA strands of different lengths and fractionated this mixture with gel electrophoresis (see chapter 4.2.2). The pattern of bands allowed allocation of deoxythymidine in the analyzed DNA. To provide sequence information of the other nucleotides Sanger used analogous terminators (ddATP, ddCTP and ddGTP). The remaining nucleotides had separate incubations. The complete sequence could be identified thanks to displays being analyzed simultaneously [62] (see figure 4.9). Today four visually different dyes are implemented, characterized by wavelength/colour of the emission happening in the base. This system allows for the products of a sequencing reaction to be fractionated in a single lane [63]. The 48-capillary 3730 DNA Analyzer (Applied Biosystems) including a sample set-up of ZMF Core-Facility Molecular Biology

was used to for illustrating purposes (Syllabus 1).

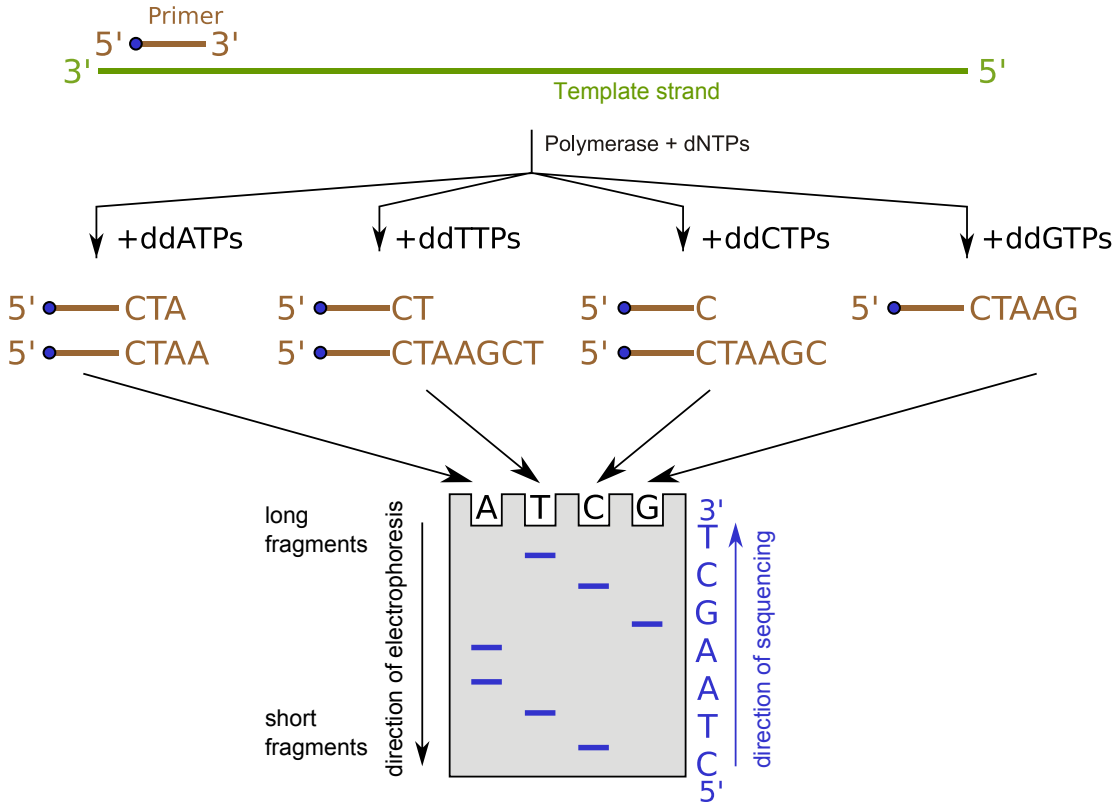

Figure 4.9: Principle of Sanger sequencing [64]

Finally electropherograms for both forward and reverse primer were analyzed by using the data visualization program SeqScape v2.5. gDNA sequence of NCBI (accession number: NM_006290, version NM_006290.2) was selected as reference sequence.

4.3 Methylation Analysis: Methylation specific PCR

Over the years, numerous PCR-based methods have been introduced to check DNA methylation [65]. Considering the pros and cons the methylation specific PCR was chosen for this project. James G. Herman came to the conclusion that MSP can detect 0.1% methylated template in a sample usually unmethylated [66]. Using a nested approach, sensitivity of MSP might rise to 0.0002% [65].

In principle all epigenetic information gets lost during PCR, because the DNA polymerase doesn't detect the difference between methylated and unmethylated DNA. This requires a modification of DNA retaining methylation information after PCR. Treatment with sodium bisulfite is used to initiate the process.

4.3.1 Sodium bisulfite treatment

Sodium bisulfite treatment with low pH and set to high temperatures causes a chemical reaction of single-stranded DNA. This mutagen brings about a rapid conversion from Cytosine to Uracil (Fig. 4.10). Methylated cytosines on the other hand are more resistant to this reaction and keep their cytosine form (Fig. 4.11).

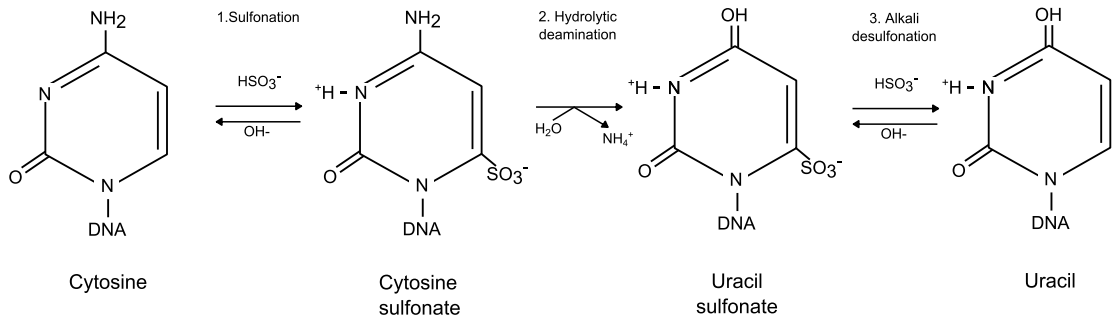

Figure 4.10: Reactions of DNA bases with sodium bisulfite: 1. Sulfonation at the carbon-6 position of cytosine, a process inhibited by methylation (methyl group on carbon-5 position) 2. Irreversible hydrolytic deamination at the carbon-4 position results in uracil sulfonate 3. Desulfonation under alkaline conditions to generate uracil

Provided favored conditions, sodium bisulfite converts 99% of cytosine residues [68] whereas on same conditions only 2-3% of 5-methylcytosine residues are converted [67]. This various characteristics may reason to the electron donating properties of the attaching methyl- group in methylated case, allowing sodium bisulfite (HSO_3-) to sulfonate at carbon-6 position of cytosine [67].

Bisulfite treatment additionally damages pyrimidine sites during reaction [69]. However, gene analyses is possible even up to the point where the degradation level gets critical, due to the fact that PCR amplifies the remaining sample.

Conclusion: Bisulfite treatment of DNA produces different sequences, depending on

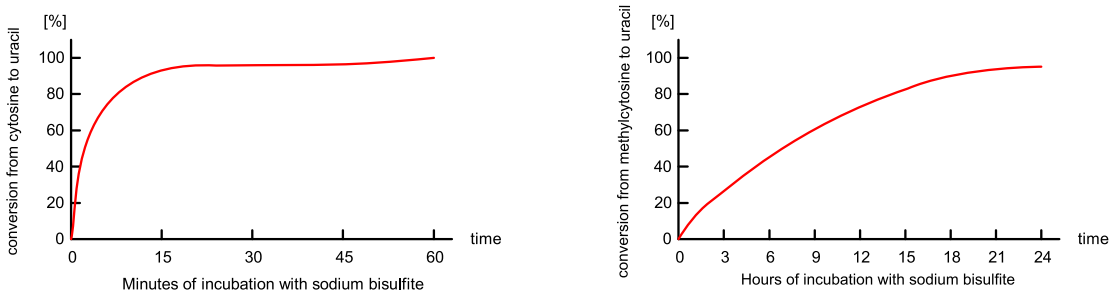

Figure 4.11: Comparison of conversion between cytosine and methylcytosine [67]

the methylation status. Bisulfite treatment was conducted with $MethylCode^{TM}$ Bisulfite Conversion Kit as described by Invitrogen Life technologies.

MSP takes advantage of this sequence alteration including bisulfite treatment shown in figure 4.12 by using different primers in order to distinguish between methylated and unmethylated DNA.

4.3.2 Primer design

The challenge in designing primers is to come up with sufficient CpG pairs in the promoter region to reassure discrimination in PCR between methylated and unmethylated DNA. Furthermore it is necessary to choose areas containing frequent cytosines to differentiate unmodified from modified DNA. Methyl Primer Express® Software v1.0 was used to achieve that goal. CpG islands in promoter region of A20/TNFAIP3 were found around the transcription initiation site (Fig. 4.13).

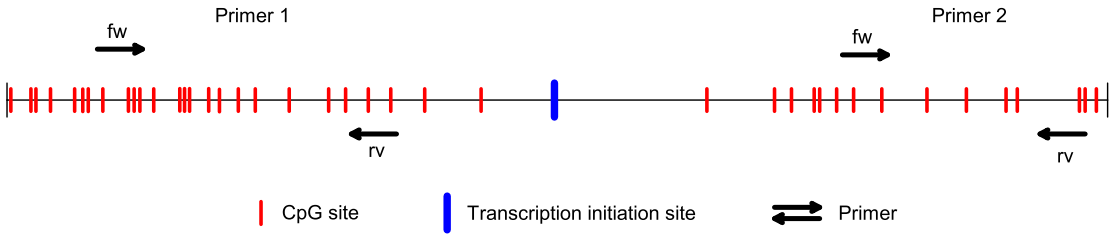

Figure 4.13: MSP Primer design: Based on arrangement of CpGs around the transcription initiation site of gene A20/TNFAIP3 two primer sets were used (see chapter 3.6.3) to detect methylation

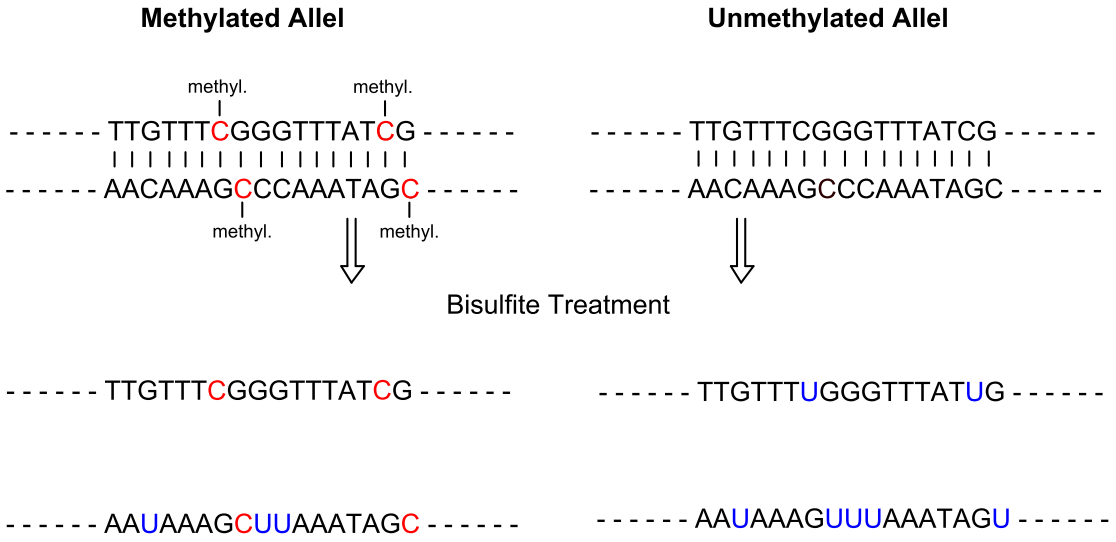

Figure 4.12: Difference between methylated and unmethylated sequence after bisulfite treatment: Those two sequences are nearly identical, only differentiating in the epigenetic modification of the methylated allele. After sodium bisulfite treatment two different sequences are achieved caused by conversion of cytosine to uracil compared to the perpetuation of cytosine in methylated case

4.3.3 Amplification - Methylation specific PCR

All Richter samples were amplified and checked separately with methylated and unmethylated primers. After unmethylated cytosines are converted to uracil using bisulfite treatment, uracil is amplified to thymidine by PCR. Only one PCR can be successful (with methylated or unmethylated primers), due to different sequences through bisulfite treatment. Depending on the methylation status of the respective sample only one primer (methylated or unmethylated) is suitable (see fig. 4.15). For every run two control DNA sets were included: $CpGenome^{TM}$ Universal Unmethylated DNA set and $CpGenome^{TM}$ Universal Methylated DNA (Millipore). After testing different polymerases and mixing ratios, reaction mixture of table 4.3 was used and taken to the thermocycler (programm see fig. 4.14).

MSP protocol	
10x PCR Buffer	1.2 µl
Primer forward (100pmol)	0.6 µl
Primer reverse (100pmol)	0.6 µl
dNTPs (10mM)	0.32µl
TAQ Polymerase	0.2 µl
Aqua dest.	15.08 µl
DNA	2 µl
Total Volume.	20 µl

Table 4.3: MSP protocol for 2 µl DNA

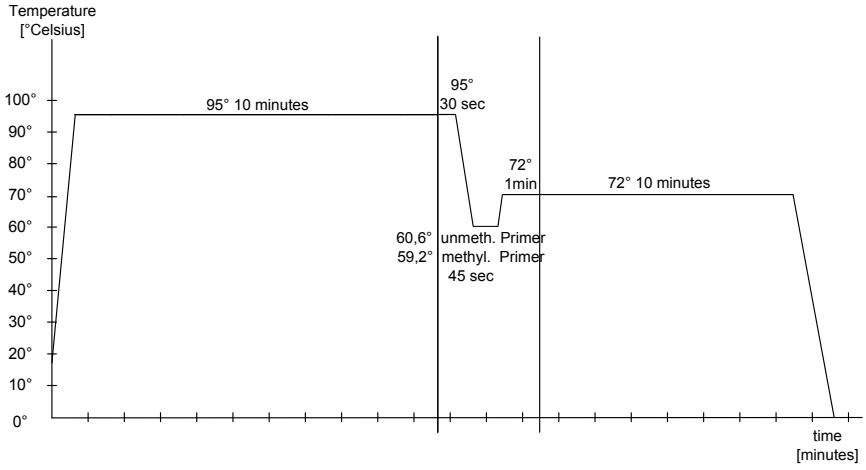

Figure 4.14: MSP program: 95° DNA denaturation, 59.2°/60.6° Primer annealing, 72° extension

As shown in fig. 4.15, examination of PCR success/methylation status is performed by gel electrophoresis afterwards (chapter 4.2.2 3% agarose gel, 100 bp ladder).

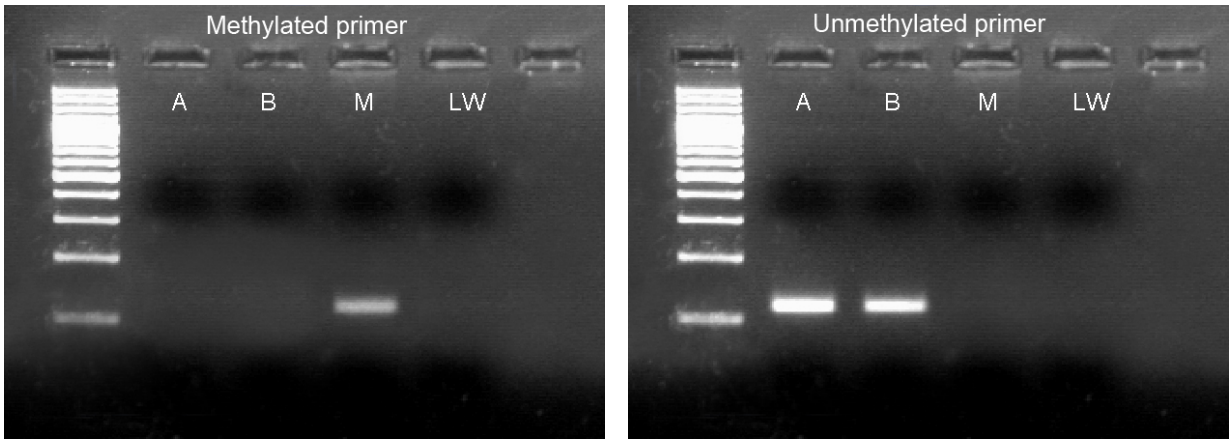

(a) PCR with methylated primers amplified sample M (methylated) but did not amplify sample A/B (unmethylated)

(b) PCR with unmethylated primers amplified sample A/B (unmethylated) but did not amplify sample M (methylated)

Figure 4.15: MSP checkgel: **A:** universal unmethylated DNA of human genomic DNA **B:** universal unmethylated DNA isolated from human fetal cell line **M:** universal methylated DNA, enzymatically methylated **LW:** non-template control

4.4 Deletion analysis: Real time PCR

The highly sensitive real time PCR (RT PCR) using the fluorescent SYBR green intercalating double stranded DNA was employed to screen for deletions in A20 locus. The DNA-dye complex absorbs blue light ($\lambda_{max} = 497nm$) and emits green light ($\lambda_{max} = 520nm$). Compared to normal PCR, RT-PCR allows to measure amplification of the product after each cycle. This is due to the fluorescence signal being quantified of SYBR green which correlates to amplification rate. SYBR green detects any double stranded DNA (contaminating DNA, primer dimers, PCR products from misannealed primer). That's why a melting curve determination was included in every run.

In order to eliminate cross contamination of reagents and surfaces, a non-template control (NTC) was applied. Beyond that a negative control (normal A20 expression) was included. For normalization two housekeeping genes (HKG), ribonuclease P RNA component H1 (RPPH1) and telomerase reverse transcriptase (TERT) were used. Furthermore every real time PCR plate contained genomic DNA of a cell line serial dilution (0%, 50%, 70%, 90% and 100%). KM-H2 cell line was mixed with UH3 cell line as demonstrated in table 4.4.

%	KM-H2	UH3
0	-	$5 \cdot 10^6$
50	$2.5 \cdot 10^6$	$2.5 \cdot 10^6$
70	$3.5 \cdot 10^6$	$1.5 \cdot 10^6$
90	$4.5 \cdot 10^6$	$5 \cdot 10^5$
100	$5 \cdot 10^6$	-

Table 4.4: Serial dilution of KM-H2 and UH3 with a total density of $5 \cdot 10^6$ cells in each tube

KM-H2 cell line has biallelic TNFAIP3 deletion in exon 3, 4, 5 and exon 6 [29]. UH3 cells don't two alleles of A20 and are immortalized human peripheral blood B cells. Therefore genomic DNA of UH3 was used as a calibrator.

All reactions were performed in triplicates and the whole measurement was carried out twice to have the results confirmed. Mixing ratio of table 4.5 was used with RT PCR program showed in fig. 4.16.

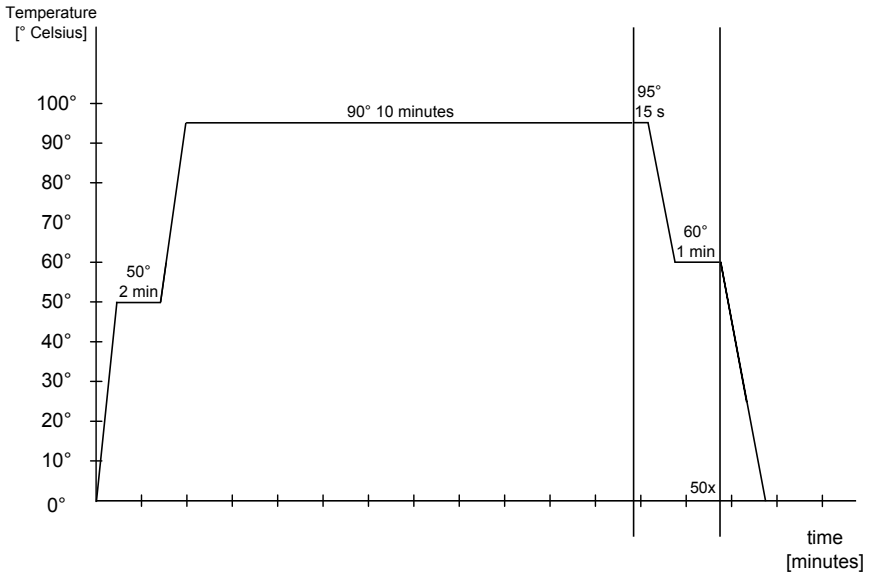

Figure 4.16: Real time cycling protocol: 50°/90° DNA denaturation, 60° Primer annealing and elongation

real time PCR protocol	
SYBR green	12.5 µl
Primer forward/reverse (1 mmol/l)	6.25 µl
Template (cell line DNA)	12.5 ng
Aqua dest.	x µl
Total Volume.	25 µl

Table 4.5: Depending on the template‘s volume and to achieve an absolute concentration of 12.5 ng, x µl aqua dest. was added to obtain a total volume of 25 µl

4.4.1 Relative quantification - The $2^{-\Delta\Delta C_T}$ method

A measure of quantification is the so called threshold cycle (C_T). This value corresponds to the number of PCR cycles required to reach a defined level of fluorescence. On crossing point every reaction vessel contains the same amount of newly synthesized DNA. Relative quantification refers number of DNA copies of a target gene to a housekeeping gene. Tissue- and matrix- effects, mistakes of real time PCR inside an experimental sample and differing extraction efficiency equally affect both the target- and housekeeping- gene abolishing each other in the following calculations. The C_T was used to quantify the DNA copy number in the samples. The mean of C_T values of RPPH1 gene and of the TERT gene was subtracted from the A20 C_T value. This difference was the ΔC_T value. The ΔC_T of the calibrator was then subtracted from the ΔC_T of the sample. This difference is called $\Delta\Delta C_T$. The results are expressed as relative units based on calculation $2^{-\Delta\Delta C_T}$, which gives the gene copy number of target gene normalized to the HKT and relative to the calibrator (UH3) [70].

Chapter 5

Results

5.1 Mutational analysis

All coding exons (exon 2 - exon 9) of A20 were tested for mutations in 16 Richter samples via DNA Sanger sequencing (see chapter 4.2). Since single base pair substitutions frequently occurred at consensus splice donor sites in other lymphoid malignancies [31], also exon-intron junctions were examined. Further nine DLBCL samples were analyzed to determine the mutational pattern in coding exons and splice sites of TNFAIP3. Neither Richter syndrome nor DLBCL displayed any mutation in TNFAIP3.

RS sample ID	Exon 2	Exon 3	Exon 4	Exon 5	Exon 6	Exon 7	Exon 8	Exon 9
R2	-	-	-	-	-	-	-	-
R3	-	-	-	-	-	-	-	-
R4	-	-	-	-	-	-	-	-
R5	-	-	-	-	-	-	-	-
R7	-	-	-	-	-	-	-	-
R9	-	-	-	-	-	-	-	-
R11	-	-	-	-	-	-	-	-
R12	-	-	-	-	-	-	-	-
R13	-	-	-	-	-	-	-	-
R16	-	-	-	-	-	-	-	-
R18	-	-	-	-	-	-	-	-
R20	-	-	-	-	-	-	-	-
R24	-	-	-	-	-	-	-	-
R25	-	-	-	-	-	-	-	-
R26	-	-	-	-	-	-	-	-
R27	-	-	-	-	-	-	-	-

Table 5.1: Results of the direct sequencing of 16 Richter samples. "-" denotes: no mutation

DLBCL sample ID	Exon 2	Exon 3	Exon 4	Exon 5	Exon 6	Exon 7	Exon 8	Exon 9
DL9	-	-	-	-	-	-	-	-
DL10	-	-	-	-	-	-	-	-
DL11	-	-	-	-	-	-	-	-
DL12	-	-	-	-	-	-	-	-
DL13	-	-	-	-	-	-	-	-
DL14	-	-	-	-	-	-	-	-
DL15	-	-	-	-	-	-	-	-
DL22	-	-	-	-	-	-	-	-
DL23	-	-	-	-	-	-	-	-

Table 5.2: Results of the direct sequencing of 9 DLBCL samples. "-" denotes: no mutation

5.2 Deletional analysis

Exon 4 and 6 of A 20 were screened in all 16 Richter samples by real time PCR. To calculate relative changes in gene expression determined by the real-time experiment the $2^{-\Delta\Delta C_P}$ method was used as described in chapter 4.4.1. The experiments were carried out twice and an average value of both measurements and standard deviation were calculated. As described earlier a serial dilution (0%, 50%, 70%, 90% and 100%) generated by mixing homozygously deleted and non-deleted cell line DNA with increasing amounts of A20 DNA exhibiting deletions in exons 4 and 6 was included in all experiments in order to further increase the sensitivity of the experimental approach. Results are summarized in table 5.3. With a cut off $2^{-\Delta\Delta C_P} =< 0.7$ six out of 16 samples (37.5%) showed monoallelic deletions in the A20 locus.

Richter sample	$2^{-\Delta\Delta C_P}$ Exon 4	$2^{-\Delta\Delta C_P}$ Exon 6	**Richter sample**	$2^{-\Delta\Delta C_P}$ Exon 4	$2^{-\Delta\Delta C_P}$ Exon 6
R2	0.656192072	0.69109244	R13	0.656933614	0.62149707
R3	0.825811891	0.79642761	R16	0.422681319	0.42075298
R4	0.883305218	0.72047195	R18	0.704583512	0.59482824
R5	0.760748608	0.70803711	R20	0.678964378	0.67589509
R7	0.727701585	0.66509021	R24	0.812793431	0.72984813
R9	0.628728114	0.53985068	R25	0.53369585	0.47650961
R11	0.820854145	0.68357427	R26	0.73726317	0.62786259
R12	0.724540693	0.62160589	R27	0.681471454	0.67774374

Table 5.3: Results of the deletional analysis of A20 by real time PCR in 16 Richter samples

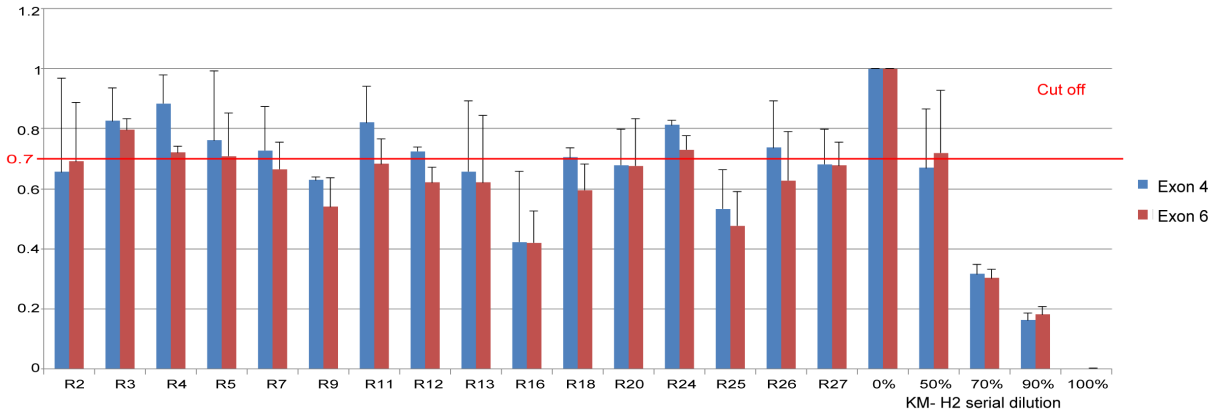

Figure 5.1: Diagram of A20 deletions: Abscissa shows all Richter samples with both exons and dilution series, the ordinate axis illustrates the different $2^{-\Delta\Delta C_P}$ values

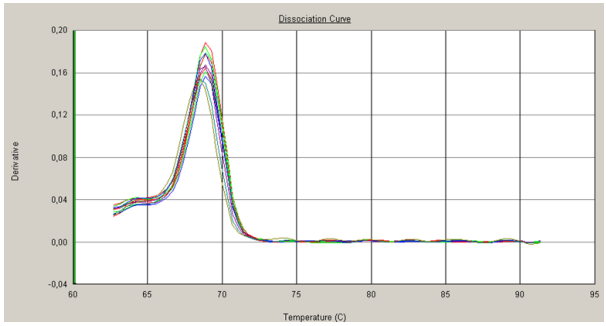

(a) Exon 4

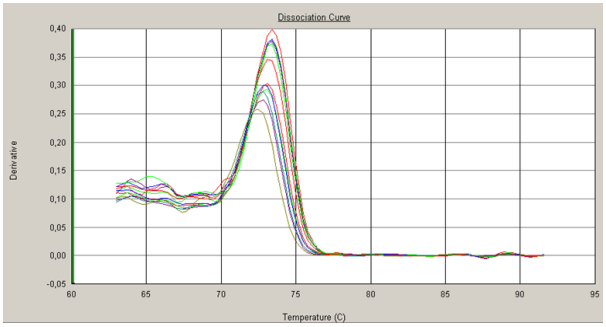

(b) Exon 6

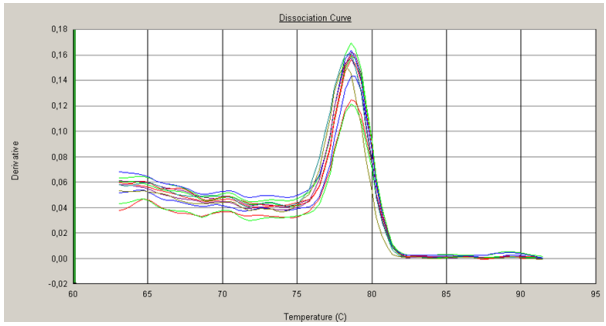

(c) TERT

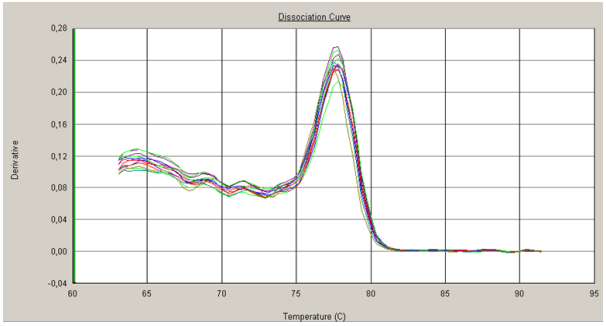

(d) RPPH1

Figure 5.2: Dissociation curve of RT PCR (Exon 4, Exon 6, TERT, RPPH1) shows one peak demonstrating the specificity of the PCR product

5.3 Promoter methylation analysis

16 RS samples were analyzed by MSP to identify promoter methylation in the A20 gene. After bisulfite treatment, the promoter sequence had changed as a result of the conversion reaction. The forward primer 1 binds twice to DNA sequence as described in fig. 5.3.

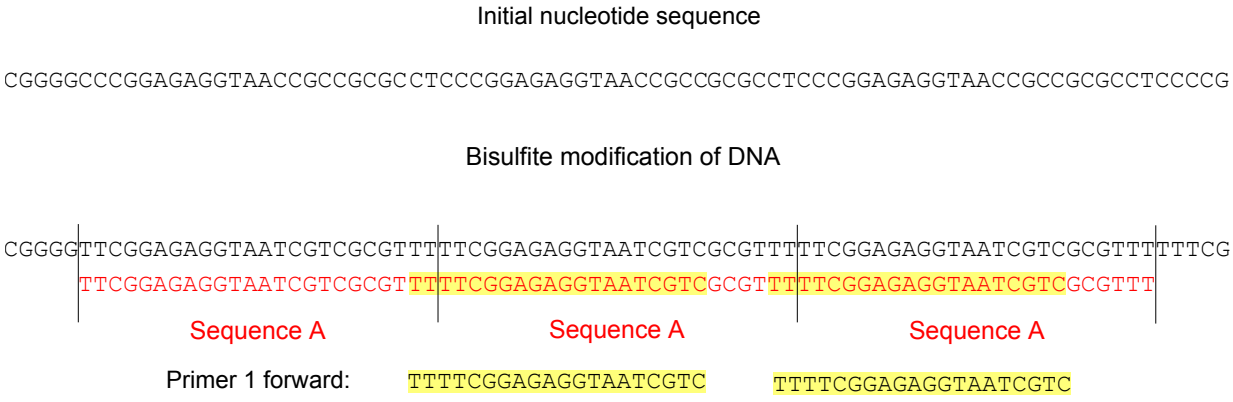

Figure 5.3: Repeating sequence by bisulfite treatment: Three equal DNA sequences (sequence A) follow each other. Primer 1 binds to the overlap area and after PCR reaction two amplicons with different length (118 bp and 142 bp) occur explaining the double bands in the gel electrophoresis (see fig. 5.4).

As shown in figures 5.4 and 5.5 none of the 16 Richter syndrome samples displayed an aberrant methylation pattern within the A20 promoter region.

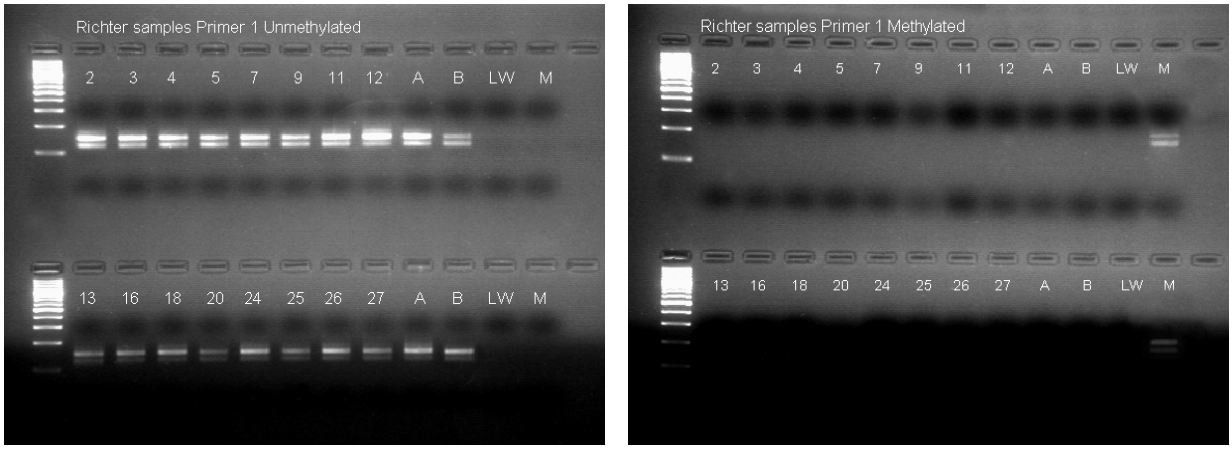

(a) (b)

Figure 5.4: Results methylation Primer 1: (a) Primer 1 unmethylated: only unmethylated samples produced bands in the gel (b) Primer 1 methylated: only methylated samples produced bands in the gel. Richter samples 2-27, **A:** universal unmethylated DNA of human genomic DNA **B:** universal unmethylated DNA isolated from human fetal cell line **M:** universal methylated DNA, enzymatically methylated **LW:** non-template control

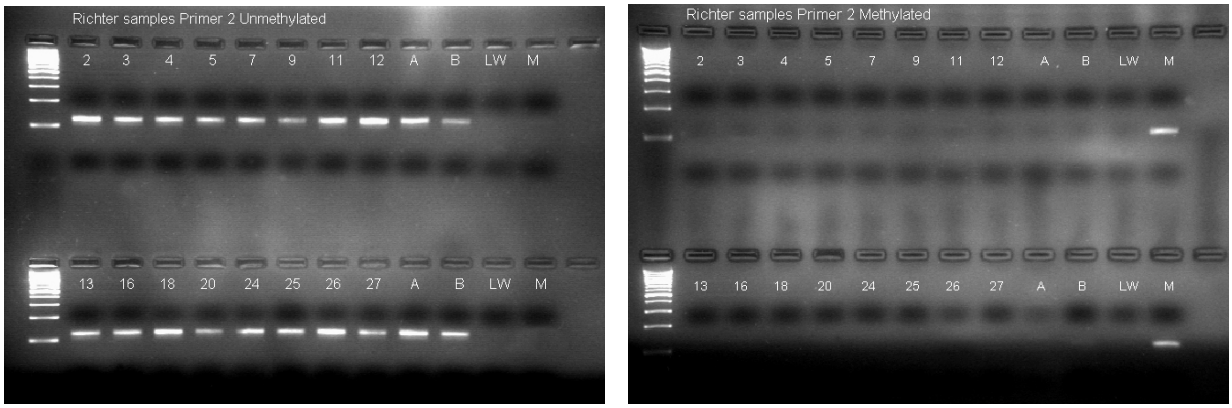

(a) (b)

Figure 5.5: Results methylation Primer 2: (a) Primer 2 unmethylated: only unmethylated samples produced bands in the gel (b) Primer 2 methylated: only methylated samples produced bands in the gel. Richter samples 2-27, **A:** universal unmethylated DNA of human genomic DNA **B:** universal unmethylated DNA isolated from human fetal cell line **M:** universal methylated DNA, enzymatically methylated **LW:** non-template control

Chapter 6

Discussion

Several lymphomas subtypes (Hodgkin disease, MALT lymphoma, DLBCL) [71] display inactivating somatic mutations in the A20 locus, leading to constitutive activation of the $NF-\kappa B$ pathway. The aim of the study was to clarify whether the disruption of the $NF-\kappa B$ pathway by inactivation of the A20 gene is similarly altered in the transformation to Richter syndrome.

6.1 Mutational analysis - RS/DLBCL

Previous studies revealed mutations of A20 in 2% of GCB-DLBCL and up to 24% in ABC-DLBCL subtypes [72]. One publication by Compagno investigating 101 DLBCL samples yielded a mutation frequency of 13.9% [4]. On the contrary results of our mutational analysis in 9 DLBCL revealed no mutation possibly indicating geographic variation/heterogeneity in the molecular pathogenesis among different sample sets. However, DLBCL sample size was too low to draw any definitive conclusions. None of 16 RS samples harboured a mutation of the tumor suppressor gene A20/TNFAIP3 indicating that inactivation of A20 by sequence alterations seems to play a minor role.

6.2 Deletion analysis

Chromosome band 6q deletion is an abundant genomic alteration in multiple NHL subtypes such as MALT lymphoma [73] [31], marginal zone B-cell lymphoma [33], mantle cell lymphoma [31] [30], Waldenström's macroglobulinemia [34], follicular lymphoma [31], ATLL [31], NK-cell lymphoma [31], Burkitt lymphoma [31] and DLBCL [31]. Honma et al

identified A20 as primary target in these cases [31]. Mono-or biallelic deletions have also been identified as frequent mechanism of inactivation of the A20 locus.

In our study real time PCR was used to quantify mono- or biallelic losses in A20 gene. With a cut off at $2^{-\Delta\Delta C_P} =< 0.7$ six out of 16 RS samples (=37%) showed a deletion. If confirmed by an alternative method (i.e. iFISH or immunohistochemistry) these results suggest a putative tumor suppressing effect of A20 in a significant fraction of RS patients.

6.3 Promoter Methylation analysis

Inactivation mechanisms other than mutation or genomic deletion may affect transformation to RS and several studies demonstrated a correlation of the A20 expression level with the promoter methylation status of several lymphoma entities [31]. Thus, promoter methylation of A20 was carried out but was unmethylated in all RS samples. Methylation seems to be of minor significance in lymphomagenesis of RS.

In conclusion mutational analysis and promoter hypermethylation of the CpG islands of A20 revealed no sequence alterations or aberrant methylation pattern. Hence, inactivation by mutation or epigenetic mechanisms seems to be of minor importance for the transformational process to Richter syndrome. However, the gene copy number assay using real time PCR revealed 7 deletions (=37%) within the A20 locus. If confirmed by a complementary method these results indicate that deletions rather than mutations seems to be involved in the molecular pathogenesis of Richter syndrome and may therefore represent a major contributor to lymphomagenesis in this NHL subtype.

Bibliography

[1] Maurice N. Richter. *Generalized reticular cell sarcoma of Lymph nodes associated with lymphatic leukemia.* The American Journal of Pathology, 1928.

[2] Davide Rossi and Gianluca Gaidano. *Richter syndrome: molecular insights and clinical perspectives.* Hematological Oncology, 2009.

[3] Lenz G, Wright GW, Emre NC, Kohlhammer H, Dave SS, Davis RE, Carty S, Lam LT, Shaffer AL, Xiao W, Powell J, Rosenwald A, Ott G, Muller-Hermelink HK, Gascoyne RD, Connors JM, Campo E, Jaffe ES, Delabie J, Smeland EB, Rimsza LM, Fisher RI, Weisenburger DD, Chan WC, and Staudt LM. *Molecular subtypes of diffuse large B-cell lymphoma arise by distinct genetic pathways.* Proc Natl Acad Sci U S A, 2008.

[4] Mara Compagno, Wei Keat Lim, Adina Grunn, Subhadra V. Nandula, Manisha Brahamachary, Qiong Shen, Francesco Bertoni, Maurilio Ponzoni, M. Marta Scandurra, Andrea Califano, Govind Bhagat, Amy Chadburn, Riccardo Dalla-Favera, and Laura Pasqualucci. *Mutations of multiple genes cause deregulation of $NF-\kappa B$ in diffuse large B-cell lymphoma.* Nature, 2009.

[5] Staudt Louis M. and Dave Sandeep. *The biology of human lymphoid malignancies revealed by gene expression profiling.* Adv. Immunol., 2005.

[6] Dominic Fong, Alexandra Kaiser, Gilbert Spizzo, Guenther Gastl, and Alexandar Tzankov. *Hodgkin's disease variant of Richter's syndrome in chronic lymphocytic leukaemia patients previously treated with fludarabine.* BJH, 2004.

[7] Stefano Molica. *A systematic review on Richter syndrome: whati is the published evidence?* Leukemia and Lymphoma, 2010.

[8] Mauro FR., Foa R., Giannarelli D., Cordone I., Crescenzi S., Pescarmona E., Sala R., Cerretti R., and Mandelli F. *Clinical characteristics and outcome of young chronic lymphocytic leukemia patients: a single institution study of 204 cases.* Blood, 1999.

[9] Naoya Nakamura and Masafumi Abe. *Richter syndrome in B-cell chronic lymphocytic leukemia.* Pathology International, 2003.

[10] Lee A, Skelly ME, Kingma DW, and Medeiros LJ. *B-cell chronic lymphocytic leukemia followed by high grade T-cell lymphoma. An unusual variant of Richter's syndrome.* American journal of Clinical Pathology, 1995.

[11] Marta Scandurra, Davide Rossi, Clara Deambrogi, Paola MV Rancoita, Ekaterina Chigrinova, Michael Mian, Michaela Cerri, Silvia Rasi, Elisa Sozzi, Francesco Forconi, Maurilio Ponzoni, Santiago M Moreno, Miguel A Piris, Giorgio Inghirami, Emanuele Zucca, Valter Gattei, Andrea Rinaldi, Ivo Kwee Gianluca Gaidano, and Francesco Bertoni. *Genomic profiling of Richters syndrome: recurrent lesions and differences with de novo diffuse large B-cell lymphomas.* Hematological Oncology, 2010.

[12] Cuneo A, de Angeli C, Roberti MG, Piva N, Bigoni R, Gandini D, Rigolin GM, Moretti S, Cavazzini P, del Senno L, and Castoldi G. *Richters syndrome in a case of atypical chronic lymphocytic leukaemia with the t(11;14)(q13;q32): role for a p53 exon 7 gene mutation.* Br J Haematol, 1996.

[13] Pinyol M, Cobo F, Bea S, Jares P, Nayach I, Fernandez PL, Montserrat E, Cardesa A, and Campo E. *p16(INK4a) gene inactivation by deletions, mutations, and hypermethylation is associated with transformed and aggressive variants of non-Hodgkin's lymphomas.* Blood, 1998.

[14] Apostolia-Maria Tsimberidou and Michael J. Keating. *Richter syndrome: Biology, Incidence, and Therapeutic Strategies.* American Cancer Society, 2004.

[15] Richard M. Locksley, Nigel Killeen, and Michael J. Lenardo. *The TNF and TNF Receptor Superfamilies: Integrating Mammalian Biology.* Cell Press, 2001.

[16] Vishva M. Dixit, Sean Green, Vidya Sarma, Lawrence B. Holzman, Frederick W. Wolf, Karen O'Rourcke, Peter A. Ward, Edward V. Prochownik, and Rory M. Marks. *Tumor Necrosis Factor- alpha Inductopm of Novel Gene Products in Human Endothelial Cells Including a Macrophage-specific Chemotaxin.* The Journal of Biological Chemistry, 1990.

[17] Yekta Dowlati, Nathan Herrmann, Walter Swardfager, Helena Liu, Lauren Sham, Elyse K. Reim, and Krista L. Lanctôt. *A Meta-Analysis of Cytokines in Major Depression.* Biol. Psychiatry, 2010.

[18] Walter Swardfager, Krista Lanctôt, Lana Rothenburg, Amy Wong, Jaclyn Cappell, and Nathan Herrmann. *A Meta-Analysis of Cytokines in Alzheimers Disease.* Biol. Psychiatry, 2010.

[19] Keiichiro Honma, Shinobu Tsuzuki, Masao Nakagawa, Sivasundaram Karnan, Yoshifusa Aizawa, Won Seog Kim, Yoon-Duk Kim, Young-Hyeh Ko, and Masao Seto. *TNFAIP3 is the Target Gene of Chromosome Band 6q23.3-q24.1 Loss in Ocular Adnexal Marginal Zone B Cell Lymphoma.* Genes, Chromosomes and Cancer, 2008.

[20] Ranjan Sen and David Baltimore. *lnducibility of K lmmunoglobulin Enhancer-Binding Protein NF-KB by a Posttranslational Mechanism.* Cell, 1986.

[21] Michael Karin and Yinon Ben-Neriah. *PHOSPHORYLATION MEETS UBIQUITINATION: The Control of NF-KB Activity.* Annual Review of Immunology, 2000.

[22] Karen Heyninck and Rudi Beyaert. *A20 inhibits NF-KB activation by dual ubiquitin-editing functions.* TRENDS in Biochemical Sciences, 2005.

[23] Momoko Nishikori. *Classical and Alternative NF-KB Activation Pathways and their Roles in Lymphoid Malignancies.* J. Clin. Ex. Hematopathol., 2005.

[24] Paul C. Evans, Huib Ovaa, Maureen Hamon, Peter J. Kilshaw, Svetlana Hamm, Stefan Bauer, Hidde L. Ploegh, and Trevor Smith. *Zinc-finger protein A20, a regulator of inflammation and cell survival, has de-ubiquitinating activity.* Biochemistry, 2004.

[25] Marco Klinkenberg, Sofie Van Huffel, Karen Heyninck, and Rudi Beyaert. *Functional redundancy of the zinc ¢ngers of A20 for inhibition of NF-KB activation and protein-protein interactions.* FEBS Letters, 2001.

[26] Su-Chang Lin, Jee Y. Chung, Betty Lamothe, Kanagalaghatta Rajashankar, Miao Lu, Yu-Chih Lo, Amy Y. Lam, Bryant G. Darnay, and Hao Wu. *Molecular Basis for the Unique Deubiquitinatinf of the NF-KB Inhibitor A20.* J. Mol. Biol., 2007.

[27] David L Boone, Emre E Turer, Eric G Lee, Regina-Celeste Ahmad, Matthew T Wheeler, Colleen Tsui, Paula Hurley, Marcia Chien, Sophia Chai, Osamu Hitotsumatsu,

Elizabeth McNally, Cecile Pickart, and Averil Ma. *The ubiquitin-modifying enzyme A20 is required for termination of Toll-like receptor responses.* Nature immunology, 2004.

[28] Roland Schmitz, Martin-Leo Hansmann, Verena Bohle, Jose Ignacio Martin-Subero, Sylvia Hartmann, Gunhild Mechtersheimer, Wolfram Klapper, Inga Vater, Maciej Giefing, Stefan Gesk, Jens Stanelle, Reiner Siebert, and Ralf Küppers. *TNFAIP3 (A20) is a tumor suppressor gene in Hodgkin lymphoma and primary mediastinal B cell lymphoma.* Journal of Experimental Medicine, 2009.

[29] Motohiro Kato, Masashi Sanada, Itaru Kato, Yasuharu Sato, Junko Takita, Kengo Takeuchi, Akira Niwa, Yuyan Chen, Kumi Nakazaki, Junko Nomoto, Yoshitaka Asakura, Satsuki Muto, Azusa Tamura, Mitsuru Iio, Yoshiki Akatsuka, Yasuhide Hayashi, Hiraku Mori, Takashi Igarashi, Mineo Kurokawa, Shigeru Chiba, Shigeo Mori, Yuichi Ishikawa, Koji Okamoto, Kensei Tobinai, Hitoshi Nakagama, Tatsutoshi Nakahata, Tadashi Yoshino, Yukio Kobayashi, and Seishi Ogawa. *Frequent inactivation of A20 through gene mutation in B-cell lymphomas.* Nature, 2009.

[30] Thelander EF, Ichimura K, Corcoran M, Barbany G, Nordgren A, Heyman M, Berglund M, Mungall A, Rosenquist R, Collins VP, Grandér D, Larsson C, and Lagercrantz S. *Characterization of 6q deletions in mature B cell lymphomas and childhood acute lymphoblastic leukemia.* Leuk. Lymphoma, 2008.

[31] Keiichiro Honma, Shinobu Tsuzuki, Masao Nakagawa, Hiroyuki Tagawa, Shigeo Nakamura, Yasuo Morishima, and Masao Seto. *TNFAIP3/A20 functions as a novel tumor suppressor gene in several subtypes of non-Hodgkin lymphomas.* Lymphoid neoplasia, 2008.

[32] Chanudet E, Huang Y, Ichimura K, Dong G, Hamoudi RA, Radford J, Wotherspoon AC, Isaacson PG, Ferry J, and M-Q Du. *A20 is targeted by promoter methylation, deletion and inactivating mutation in MALT lymphoma.* Leukemia, 2010.

[33] Urban Novak, Andrea Rinaldi, Ivo Kwee, Subhadra V. Nandula, Paola M. V. Rancoita, Mara Compagno, Michaela Cerri, Davide Rossi, Vundavalli V. Murty, Emanuele Zucca, Gianluca Gaidano, Riccardo Dalla-Favera, Laura Pasqualucci, Govind Bhagat, and Francesco Bertoni. *The $NF-\kappa B$ negative regulator TNFAIP3 (A20) is inactivated by somatic mutations and genomic deletions in marginal zone lymphomas.* Blood, 2009.

[34] Braggio E, Keats JJ, Leleu X, Van Wier S, Jimenez-Zepeda VH, Valdez R, Schop RF, Price-Troska T, Henderson K, Sacco A, Azab F, Greipp P, Gertz M, Hayman S, Rajkumar SV, Carpten J, Chesi M, Barrett M, Stewart AK, Dogan A, Bergsagel PL, Ghobrial IM, and Fonseca R. *Identification of copy number abnormalities and inactivating mutations in two negative regulators of nuclear factor-kappaB signaling pathways in Waldenstrom's macroglobulinemia.* Cancer Research, 2009.

[35] J.D. Watson and F.H.C. Crick. *Molecular structure of nucleic acids.* Nature, 1953.

[36] Benjamin Lewin. *Molekularbiologie der Gene.* Spektrum, 2002.

[37] Geoffrey M. Cooper. *The Cell: A Molecular Approach.* Boston University, 2000.

[38] Keith D. Robertson and Peter A. Jones. *DNA methylation: past, present and future directions.* Carcinogenesis, 2000.

[39] Colum P. Walsh, J. Richard Chaillet, and Timothy H. Bestor. *Transcription of IAP endogenous retroviruses is constrained by cytosine methylation.* Nature Amer, 1998.

[40] En Li, Caroline Beard, and Rudolf Jaenisch. *Role for DNA methylation in genomic imprinting.* Nature, 1993.

[41] Barbara Panning and Rudolf Jaenisch. *RNA and the Epigenetic Regulation of X Chromosome Inactivation.* Cell, 1998.

[42] Mary Grace Goll and Timothy H. Bestor. *Eukaryotic Cytosine Methyltransferases.* Annu. Rev. Biochem., 2005.

[43] John Hayslip and Alberto Montero. *Tumor suppressor gene methylation in follicular lymphoma: a comprehensive review.* Molecular cancer, 2006.

[44] J. T. Attwood, R.L. Yung, and B. C. Richardson. *DNA methylation and the regulation of gene transcription.* CMLS Cellular and Molecular Life Sciences, 2001.

[45] Masaki Okano, Shaoping Xie, and En Li. *Dnmt2 is not required for de novo and maintenance methylation of viral DNA in embryonic stem cells.* Oxford University Press, 1998.

[46] Masaki Okano, Shaping Xie, and En Li. *Cloning and characterization of a family of novel mammalian DNA (cytosin-5) methyltransferases.* Nature America, 1998.

[47] Masaki Okano, Daphne W. Bell, and Daniel A. Haber. *DNA Methyltransferases DNMT3a and DNMT3b are essential for de novo methylation and mammalian development.* Cell Press, 1999.

[48] Adrian P.Bird. *DNA methylation and the frequency of CpG in animal DNA.* Nucleic Acids Research, 1980.

[49] Richard D. Wood, Michael Mitchell, John Sgouros, and Tomas Lindahl. *Human DNA Repair Genes.* Analysis of Genomic Information, 2001.

[50] Melanie Ehrlich, Miguel A.Gama-Sosa, Lan-Hsiang Huang, Rose Marie Midgett, Kenneth C. Kuo, Roy A.McCune, and Charles Gehrke. *Amount and distribution of 5-methylcytosine in human DNA from different types of tissues or cells.* Nucleic Acids Research, 1982.

[51] Michael Comb and Howard M. Goodman. *CpG methylation inhibits proenkephalin gene expression and binding of the transcription factor AP-2.* Nucleic, 1990.

[52] Xinsheng Nan, Richard R. Meehan, and Adrian Bird. *Dissection of the methyl-CpG binding domain from the chromosomal protein MeCP2.* Nucleic Acids Research, 1993.

[53] Rolf Knippers. *Molekulare Genetik.* Thieme, 2006.

[54] Patrick Trojer and Danny Reinberg. *Facultative Heterochromatine: Is there a distinctive molecular signature?* Cell Press, 2007.

[55] Davide Rossi, Daniela Capello, Annunziata Gloghini, Silvia Franceschetti, Marco Paulli, Kishor Bhatia, Giuseooe Saglio, Umberto Vitolo, Stefano A. Pileri, Manel Esteller, Antonio Carbone, and Gianluca Gaidano. *Aberrant promoter methylation of multiple genes throughout the clinico-pathologic spectrum of B-cell neoplasia.* Haematologica, 2004.

[56] Randall K. Saiki, David H. Gelfand, Susanne Stoffel, Stephen J. Scharf, Russel Higuchi, Glenn T. Horn, Kary B. Mullis, and Henry A. Ehrlich. *Primer-Directed Enzymatic Amplification of DNA with a Thermostable DNA Polymerase.* Science, 1987.

[57] Michael A. Innis, Kenneth B. Myambo, David H. Gelfand, and Mary Ann D. Brown. *DNA sequencing with Thermus aquaticus DNA polymerase and direct sequencing of polymerase chain reaction-amplified DNA.* Biochemistry, 1988.

[58] Wim Gaastra. *Chemical Cleavage (Maxam and Gilbert) Method for DNA Sequence Determination.* Methods Mol Biology, 1984.

[59] Maurice R. Atkinson, Murray P. Deutscher, Arthur Kornberg, Alan F. Russel, and J. G. Moffatt. *Enzymatic Synthesis of Deoxyribonucleic Acid. XXXIV. Termination of Chain Growth by a 2´,3´- Dideoxyribonucleotide.* Biochemistry, 1969.

[60] Alice McGovern Doering, Miekie Jansen, and Seymour S. Cohen. *Polymer synthesis in killed bacteria: lethality of 2',3'-dideoxyadenosine.* Journal of Bacteriology, 1966.

[61] Keith Kretz, Walter Callen, and Valerie Hedden. *Cycle Sequencing.* Genome Research, 1994.

[62] F. Sanger, S. Nicklen, and A. R. Coulson. *DNA sequencing with chain-terminating inhibitors.* Biochemistry, 1977.

[63] Gabor L. Igloi. *Strategies for introducing non-radioactive labels during the automated sequence analysis of nucleic acids.* EJB Electronic Journal of Biotechnology, 1998.

[64] Dr. Norman Mauder. *Didesoxy-Methode.* http://de.wikipedia.org/wiki/DNA-Sequenzierung, 2009.

[65] Lasse Sommer Kristensen and Lise Lotte Hansen. *PCR based methods for detecting single locus DNA methylation biomarkers in cancer diagnostics, and response to treatment.* Clinical chemistry, 2009.

[66] James G. Herman, Jeremy R. Graff, Sanna Myöhänen, Barry D. Nelkin, and Stephen B. Baylin. *Methylation specific PCR: A novel PCR assay for methylation status of CpG islands.* Medical Sciences, 1996.

[67] Richard Y. H. Wang, Charles W. Gehrke, and Melanie Ehrlich. *Comparison of 5-methyldeoxycytidine and deoxycytidin residues.* Nucleic Acids Research, 1982.

[68] Kristen H. Taylor, Robin S. Kramer, J. Wade Davis, Juyuan Gua, Deiter J. Duff, Dong Xu, Charles W. Caldwell, and Huidong Shi. *Ultradeep bisulfite sequencing analysis of DNA methylation patterns in multiple gene promoters by 454 sequencing.* Cancer research, 2007.

[69] Kazuo Tanaka and Akimitsu Okamoto. *Degradation of DNA by bisulfite treatment.* Science Direct, 2007.

[70] Kenneth J. Livak and Thomas D. Schmittgen. *Analysis of Relative Gene Expression Data Using Real-Time Quantitative PCR and the* $2^{-\Delta\Delta c_T}$ *Method.* Applied Biosystems, 2001.

[71] Lukas P. Frenzel, Rainer Claus, Nadine Plume, Janine Schwamb, Caroline Konermann, Christian P. Pallasch, Julia Claasen, Reinhild Brinker, Bernd Wollnik, Christoph Plaas, and Clemens-Martin Wendtner. *Sustained* $NF-\kappa B$ *activity in chronic lymphocytic leukemia is independent of genetic and epigenetic alterations in the TNFAIP3 (A20) locus.* International Journal of Cancer, 2010.

[72] Manuel Montesinos-Rongen, Roland Schmitz, Anna Brunn, Stefan Gesk, Julia Richter, Ke Hong, Otmar D. Wiestler, Reiner Siebert, Ralf Küppers, and Martina Deckert. *Mutations of CARD11 but not TNFAIP3 may activate the* $NF-\kappa B$ *pathway in primary CNS lymmphoma.* Acta Neuropathol., 2010.

[73] Chanudet E, Ye H, Ferry J, Bacon CM, Adam P, Müller-Hermelink HK, Radford J, Pileri SA, Ichimura K, Collins VP, Hamoudi RA, Nicholson AG, Wotherspoon AC, Isaacson PG, and Du MQ. *A20 deletion is associated with copy number gain at the TNFA/B/C locus and occurs preferentially in translocation-negative MALT lymphoma of the ocular adnexa and salivary glands.* J Pathol, 2009.